

2-0

FINAL PROGRESS REPORT

for

DEVELOPMENT OF IMPROVED PLAQUE MATERIAL
FOR AEROSPACE NICKEL-CADMIUM CELLS

(17 November 1969 - 17 November 1970)

Contract No.: NAS 5-21105

Prepared by

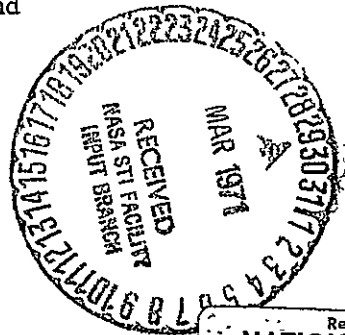
G. R. Schaer, F. Goebel,
A. H. Reed, and J. McCallum

Battelle Memorial Institute
Columbus Laboratories
505 King Avenue
Columbus, Ohio 43201

for

Goddard Space Flight Center
Greenbelt, Maryland

FACILITY FORM 602	N71 20818 (ACCESSION NUMBER)	(THRU)
	62 (PAGES)	53 (CODE)
	CR-117482 (NASA CR OR TMX OR AD NUMBER)	03 (CATEGORY)



Reproduced by
**NATIONAL TECHNICAL
 INFORMATION SERVICE**
 Springfield, Va. 22151

FINAL PROGRESS REPORT

for

DEVELOPMENT OF IMPROVED PLAQUE MATERIAL
FOR AEROSPACE NICKEL-CADMIUM CELLS

(17 November 1969 - 17 November 1970)

Contract No.: NAS 5-21105

Prepared by

G. R. Schaer, F. Goebel,
A. H. Reed, and J. McCallum

Battelle Memorial Institute
Columbus Laboratories
505 King Avenue
Columbus, Ohio 43201

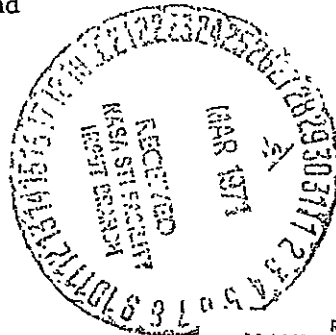
for

Goddard Space Flight Center
Greenbelt, Maryland

FACILITY FORM 602

NTI 20818
(ACCESSION NUMBER)
62
(PAGES)
CR-111482
(NASA CR OR TMX OR AD NUMBER)

(THRU)
5-3
(CODE)
03
(CATEGORY)



Case file

N71-20818

Battelle Memorial Institute • COLUMBUS LABORATORIES

505 KING AVENUE COLUMBUS, OHIO 43201 • AREA CODE 614, TELEPHONE 299-3151 • CABLE ADDRESS BATMIN

March 24, 1971

National Aeronautics and
Space Administration
Goddard Space Flight Center
Greenbelt, Maryland 20771

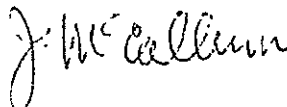
Attention Mr. Joseph M. Sherfey, Code 735

Gentlemen:

"Development of Improved Plaque Material for
Aerospace Nickel-Cadmium Cells"
Contract No. NAS5-21105

Enclosed is a copy of the final report on the subject contract NAS5-21105. As directed in the GSFC specifications S-250-P-1, 1 reproducible copy is being forwarded to the Documentation Branch, Code 256. Other copies to NASA are being distributed in accordance with the last paragraph of Article II in the contractual requirements. Remaining copies are being distributed in accordance with your approval letter dated January 21, 1971.

Yours sincerely,



John McCallum
Chief
Electrochemical Engineering
Division

JM:cs

cc: Distribution

DO NOT PHOTOGRAPH THIS PAGE

FINAL PROGRESS REPORT

for

DEVELOPMENT OF IMPROVED PLAQUE MATERIAL
FOR AEROSPACE NICKEL-CADMIUM CELLS

(17 November 1969 - 17 November 1970)

Contract No.: NAS 5-21105

Goddard Space Flight Center

Contracting Officer: P. Videnieks
Technical Officer: J. M. Sherfey

Prepared by

— G. R. Schaer, F. Goebel,
A. H. Reed, and J. McCallum

Battelle Memorial Institute
Columbus Laboratories
505 King Avenue
Columbus, Ohio 43201

for

Goddard Space Flight Center
Greenbelt, Maryland

ABSTRACT

Porous nickel electrodes have been fabricated with a honeycomb structure providing direct connection of each pore to the surface of the electrode. These electrodes are expected to extend the life of sealed nickel-cadmium cells. Procedures were developed for electroforming thin (0.2 to 0.4 mil) nickel foils with corrugations 3 to 10 mils wide, and for constructing mechanically strong honeycomb plaques from corrugated and flat nickel foils. Electrodes with five different pore sizes were fabricated and evaluated as rechargeable cadmium electrodes. Performance of the honeycomb electrodes showed a maximum capacity for pores of 4.2 mils diameter and a capacity similar to sintered nickel powder electrodes.

TABLE OF CONTENTS

	<u>Page</u>
MANAGEMENT SUMMARY	1
Objective of the Research	1
Significance of the Results	1
How NASA Can Utilize Results	2
RECOMMENDED FUTURE WORK	2
INTRODUCTION	3
EXPERIMENTAL RESULTS AND DISCUSSION	5
Program Plans	5
Task A. Approaches	6
Nickel Honeycomb Structure	6
Pore Size	10
Electroforming Mandrel Fabrication	10
Alternate Mandrel-Fabrication Methods	15
Corrugated-Foil Electroforming	16
Flat-Foil Electroforming	16
Fabricating Plaques	16
Alloy Honeycomb Structure	18
Corrugated Plaques	18
Task B. Plaque Characterization	19
Pore Size, Shape, and Internal Area	19
Flexibility of Plaques	19
Electrical Resistance	19
Task C. Plaque Impregnation	24
Honeycomb Plaque	24
Description of the Impregnation Process	26
Description of Apparatus	27
Impregnation Results	30
Electrode Formation	34
Corrugated Plaque	36
Task D. Electrochemical Evaluation of Electrode	36
Electrode-Capacity Measurements	36
Electrode Performance During Cycling	37
Temperature Effects	43
Oxygen Recombination	45
Wetting Rates of Electrodes	47

TABLE OF CONTENTS
(Continued)

	<u>Page</u>
Corrugated-Electrode Cycling	49
Plans for Life Tests	51
Electrode Fabrication	52
Life Tests	52
New Technology	54
CONCLUSIONS AND RECOMMENDATIONS	54

LIST OF TABLES

Table 1. Physical Characteristics of Honeycomb Plaques	23
Table 2. Electrical Resistance of Plaques	24
Table 3. Cycles Required to Impregnate Honeycomb Plaques	31
Table 4. Analysis of Cadmium Electrodes	33
Table 5. Calculated Amount of Plaque Pore Volumes Filled With Cd(OH) ₂	33
Table 6. Capacity of Cadmium Electrodes During Cycling Experiments	39
Table 7. Electrode Potentials as a Function of Temperature	45
Table 8. Electrode Capacity as a Function of Temperature Capacity in Ampere-Hours	46
Table 9. Rate and Amount of Wetting of Electrodes With 30 Percent KOH	48
Table 10. Absorbed Electrolyte in Electrodes	49
Table 11. Discharge Results of Cell Containing A Corrugated-Foil Electrode	50

LIST OF FIGURES

	<u>Page</u>
Figure 1. Layered Honeycomb Structure	7
Figure 2. Stacked Honeycomb Structure	8
Figure 3. Alternating Honeycomb Structure	9
Figure 4. Cutting Tool Used for Threading Mandrels	13
Figure 5. Photomicrograph of Honeycomb Plaque With 0.015 CM Pores	20
Figure 6. Photomicrograph of Honeycomb Plaque With 0.01 CM Pores	20
Figure 7. Photomicrograph of Honeycomb Plaque With 0.0076 CM Pores	21
Figure 8. Photomicrograph of Honeycomb Plaque With 0.0061 CM Pores	21
Figure 9. Honeycomb Plaque With 0.0049 CM Pores	22
Figure 10. Plaque With Coined Edge and Tab Attached by Spot Welding	25
Figure 11. Vacuum Impregnation Apparatus	28
Figure 12. Polarization Tank	29
Figure 13. Photomicrograph of Honeycomb Plaque After Eight Impregnations	35
Figure 14. Automatic Cycling Facility	38
Figure 15. Typical Charge and Discharge Curve for Sintered- Powder and Honeycomb Electrodes	42
Figure 16. Charge and Discharge Curves at 4C Rate for 0.0107 cm Honeycomb Electrode and Sintered Powder Electrode	44

DEVELOPMENT OF IMPROVED PLAQUE MATERIALS
FOR AEROSPACE NICKEL-CADMIUM CELLS

by

G. R. Schaer, F. Goebel,
A. H. Reed, and J. McCallum

MANAGEMENT SUMMARY

Objective of the Research

The objective of this development program was to provide nickel-cadmium cells with longer life by developing a new plaque material with controlled pore geometry. The plaques are expected to provide longer life electrodes for extended service in space vehicles.

Significance of the Results

Fabrication of plaques with honeycomb configurations has been accomplished with the use of electroformed flat and corrugated nickel foils. The alternate flat and corrugated foils were stacked and heat bonded, and the honeycomb block was sliced into plaques. Porosity of honeycomb plaques was about 80 percent.

A honeycomb configuration, believed to be new, was devised to provide maximum bonding area between foil layers and to resist deformation during the heat-bonding and during impregnation steps. The new configuration was obtained by alternating flat and corrugated foils and by turning the alternate corrugated foils about 30 degrees with respect to each other.

Techniques were developed for machining brass mandrels with 3- to 10-mil threads. These new techniques required polishing the threads to remove burrs and surface roughness. The polished brass mandrels were

electroplated with bright nickel and bright chromium to provide a surface from which electroformed corrugated foils could be removed easily.

Plaques were made by filling the honeycomb blocks and slicing sections from the block with a thin grinding wheel. The filler used was an epoxy resin. The epoxy was removed by dissolution in hot chromic acid solution. Slicing of plaques by EDM (Electric Discharge Machining) was also successfully accomplished but was considered too slow because 7 hours were required to make one cut.

Impregnated plaques were cycled to 100 percent depth of discharge in cells containing a single negative Pellon separator and two positive electrodes. Honeycomb plaques with 0.010-cm (4.2-mil) pores provided the largest discharge capacities, which were similar to capacities of conventional sintered-powder electrodes. Cycling was carried out with discharge currents to approximate 4C, 2C, C, C/2, and C/4 rates for the experimental electrodes.

How NASA Can Utilize Results

These results can help NASA personnel in their planning to achieve uniform, reproducible, and long-life battery components. Included in these plans should be a program to evaluate the life of cadmium electrodes made from honeycomb plaques.

RECOMMENDED FUTURE WORK

Because honeycomb electrodes were successfully made with structures that are expected to provide increased life of cadmium electrodes in nickel-cadmium cells, a program is recommended to determine the amount of improvement obtainable. Included in such a program should be optimization of the impregnation procedure to fill the honeycomb plaques with an active form of cadmium material in the optimum amount. Conventional impregnation by the method described by Fleischer^{(1)*} did not result in optimum impregnation of the plaques. Other methods such as electrolytic impregnation in aqueous

* References are listed on page (55).

cadmium nitrate should be evaluated. Honeycomb electrodes impregnated by the optimized method should be evaluated by the methods described in another section of this report for predicting life of negative cadmium electrodes.

INTRODUCTION

Although porous plaques made from sintered nickel-powder provide a practical method for making porous nickel structures of low density and high surface area, the electrodes made from such plaques are not as efficient as might be possible. About half of the active material is seldom used for producing electrical power. Utilization of active material is low partly because the pores in sintered-powder plaques are variable with respect to diameter, length, tortuosity, and direction, so that some of the active material is electrochemically unavailable under any circumstance. Part of the low utilization derives from a deliberate attempt to achieve more charge/discharge cycles by limiting depth of discharge to 50 percent or less. Another part of the low utilization is caused by the manufacturer's use of extra negative capacity so that customers may allow occasional excursions to low temperatures or to high rates of discharge. Another reason for the low utilization derives from the need to have excess uncharged $\text{Cd}(\text{OH})_2$ at the negative electrode when the end of charging is reached at the positive electrode so that hydrogen evolution is avoided in a sealed cell. Still another reason for the low utilization is caused by a well-known but somewhat mysterious fading of the capacity that was available initially.

To explain why cadmium electrodes will not deliver full capacity on short-time discharges, one hypothesis is based on the fact that electrodes made from sintered-powder plaques have variable pore sizes. A large pore in the center of a plaque which is connected to the surface by very small pores is partially isolated electrically from the system. One geometry that overcomes this feature has all pores open directly to the surface of the electrode, thereby providing a direct and uniform path for current flow.

A second hypothesis is that ampere-hour capacity is lost during cycling because the active cadmium material moves from pore to pore toward the bottom of the electrode since gravity causes the nonadherent cadmium hydroxide to settle slightly during each discharge. Movement of the active material would eventually leave some pores almost void and other pores so full of active material that electrolyte volume would be restricted and the discharge capacity limited. A structure that has noninterconnected pores is expected to prevent loss of capacity by this mechanism.

A third hypothesis predicts that capacity is lost during cycling because cadmium material moves out of large pores into small pores of electrodes made from sintered-powder plaques. Cadmium sponge metal is believed to discharge first in the large pores most accessible to current flow, producing cadmium hydroxide, a portion of which then migrates to adjacent smaller pores which contain some unused cadmium sponge metal. During the next charge, which is often an overcharge, cadmium hydroxide is reduced to sponge metal in situ. The result is that during each incomplete discharge and complete charge cycle, metal moves toward the smaller or electrically less accessible pores. A structure with pores of uniform size is expected to negate this hypothesized mechanism for loss of capacity.

To overcome these hypothesized mechanisms that lead to inefficiency of the sintered porous structure, a geometry is required to

- (1) Provide uniform pore sizes
- (2) Provide noninterconnected pores
- (3) Provide direct connection of each pore to the separator.

A honeycomb structure meets these geometric requirements. In addition, honeycomb structures can have large porosities equivalent to those of conventional sintered-powder plaques. However, to obtain a porosity of about 80 percent, the walls of the honeycomb must be relatively small in relation to the pore size. Methods for making these highly porous structures are described in the "Experimental Results and Discussion" section of this report.

EXPERIMENTAL RESULTS AND DISCUSSIONProgram Plans

The program for developing improved plaque material for increasing the life of aerospace nickel-cadmium cells was conducted with the following steps and goals:

- (1) Hypothesize shortcomings of presently available plaque material
- (2) Prepare an idealized structure to overcome these shortcomings
- (3) Construct plaques with this structure
- (4) Impregnate the plaques to make electrodes
- (5) Evaluate the electrochemical performance of the electrodes to determine if capacities are in a practical range
- (6) Propose a program for evaluating life of the new electrode structure
- (7) Compare useful life of new electrode structure with presently available electrode materials
- (8) Optimize the fabrication and impregnation systems
- (9) Devise production facilities for producing plaque materials at a minimum cost.

The program has been carried through Step 5, and plans for Step 6 have been detailed. The evaluation in Step 7 was not to be started during the current contract period.

The experimental techniques and results are arranged in this report according to tasks as follows:

Task A. ApproachesTask B. Plaque CharacterizationTask C. Plaque ImpregnationTask D. Electrochemical Evaluation of Electrodes

Task A. Approaches

Nickel Honeycomb Structure

Nickel plaques resembling a microscopic honeycomb were made from electroformed corrugated and flat foils. Many layers of these foils were stacked and held in a graphite fixture and bonded by heating in a hydrogen atmosphere to make three different honeycomb configurations. These configurations are shown in Figures 1, 2, and 3.

The structure in Figure 1 was made by alternating flat and corrugated foils so that all the corrugations were parallel. When the honeycomb structures were sintered, some shrinkage occurred because the flat foils warped when the corrugations were not adjacent to each other. Another way of explaining the warping action is to say that the corrugated foils partly nested and bent the flat foils.

The structure in Figure 2 was made by stacking corrugated foils with alternate foils turned about 30 degrees with respect to the corrugation lines. In this way, the foils could not nest. Then, after slicing the structure into 30-mil-thick plaques, each 10-mil corrugation would have at least one contact point with an adjoining corrugation. A possible advantage of this geometry is that most of the internal surface area would be available for accepting active material. However, a disadvantage is the inherent weakness of the structure because bonding between corrugated foils would be at single points. By contrast, the structure in Figure 1 was bonded along a line where each corrugation met the flat sheet.

The structure which was selected as preferred for the honeycomb plaques is shown in Figure 3. Flat and corrugated foils were stacked with every other corrugated foil turned 30 degrees. This structure provides (1) a geometry which resists distortion during the bonding, (2) a strong structure because bonding between foils is along lines instead of at a single point, and (3) a total surface area in a plaque which is higher per unit/weight because the flat foils were made thinner than the corrugated foils. The reasons for making the flat foils thinner than the corrugated foils are discussed in the Fabricating Plaques section, page (18).

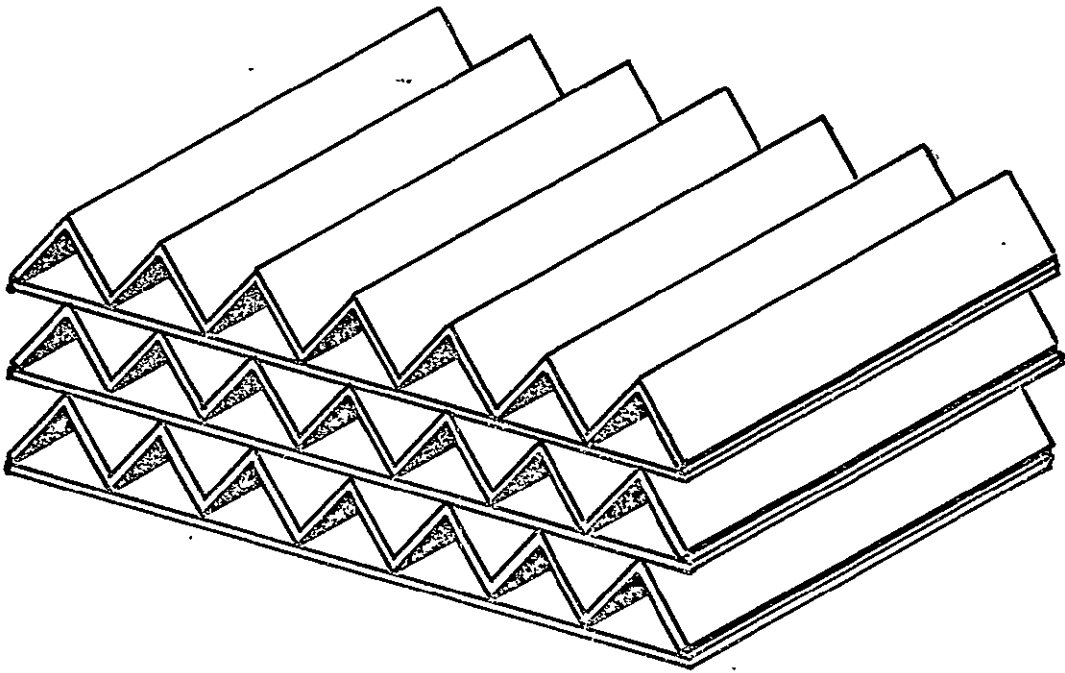


FIGURE 1. LAYERED HONEYCOMB STRUCTURE
(NOT TO SCALE)

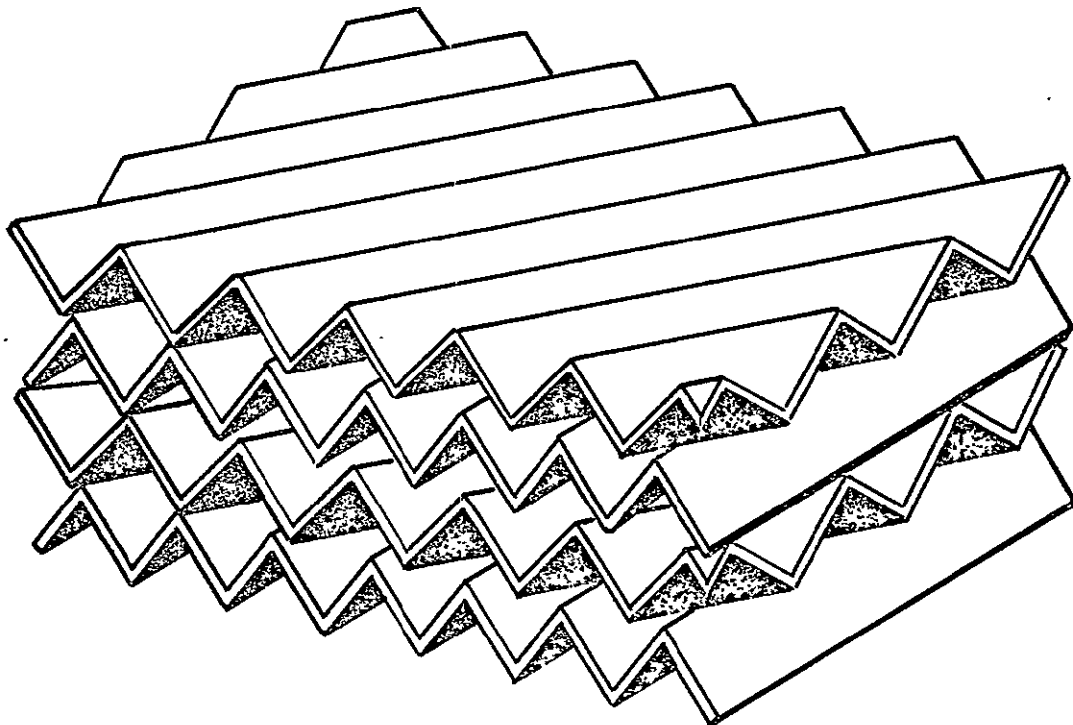


FIGURE 2. STACKED HONEYCOMB STRUCTURE
(NOT TO SCALE)

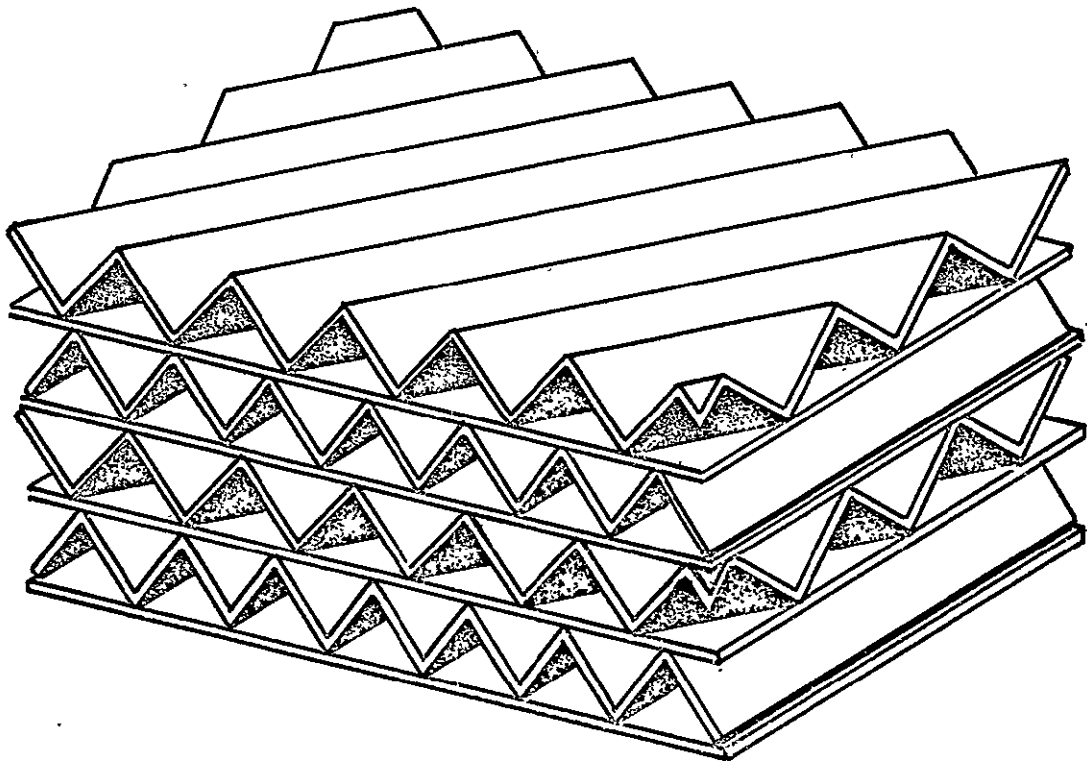


FIGURE 3. ALTERNATING HONEYCOMB STRUCTURE
(NOT TO SCALE)

Pore Size. Nickel plaques with five pore sizes were made for comparing performance with pore size after impregnating the pores with cadmium compounds. Details of the results are found in other sections of this report. Corrugated foils required for fabricating all pore sizes were electroformed. These five corrugated foils have five different peak-to-peak dimensions of approximately 0.025, 0.018, 0.013, 0.010, and 0.0080 cm. Assuming an equilateral, triangular shaped pore, the diameters of inscribed circles in these pores would measure 0.015, 0.010, 0.008, 0.006, and 0.005 cm, respectively. Such pore sizes approximate the results expected of mercury porosimeter measurements.

Electroforming Mandrel Fabrication. At the start of this program, no known method was available for making a mandrel suitable for electroforming corrugated nickel sheets thin enough and with narrow enough grooves to allow the honeycomb plaques to be assembled with the desired pore sizes. Therefore, a technique was developed for machining the necessary threads on a rod. These threads were polished and chromium plated to make the mandrels usable.

The following steps were developed to make an electroforming mandrel which could be used to make replicate corrugated foils. Details of each step are discussed in the paragraphs that follow the listing. A detailed discussion is necessary because considerable effort was needed to develop suitable techniques for fabrication.

- Step 1. Machine a 2-inch-diameter brass bar about 15 inches long to the true surface and leave a smooth finish.
- Step 2. Machine threads in the bar in one cut using a specially sharpened tool.
- Step 3. Check depth of cut with RTV silicone rubber replica.
- Step 4. File a flat side on the mandrel about 1/4 to 3/8 inch wide to provide a starting edge for removing the electroformed foils.

- Step 5. Polish the threads lightly with 600-grit abrasive paper to remove burrs from the top of the threads.
- Step 6. Polish the sides of the threads using a fine brass brush with pointed wires and a slurry of fine abrasive.
- Step 7. Clean and inspect the polished mandrel.
- Step 8. Electroplate the mandrel with bright nickel and bright chromium.
- Step 9. Apply electroplater's tape to mask the ends of the mandrel and the flattened side made in Step 4.
- Step 10. Clean the mandrel with a soft fiber brush and magnesium oxide slurry before starting the electroforming sequence (described in a following section of this report).

Step 1. Several different materials were evaluated for mandrel materials including brass, cartridge brass, electroplated bright copper, aluminum, stainless steel, and several plastics. Solid brass 70-30 bar stock was used because of its availability. Cartridge brass, which had a finer grain size, could be machined with a slightly smoother surface than the bar stock. A bright-copper electroplate* about 10 mils thick applied to a brass bar produced the smoothest machined threads of any metal. However, the threads still required polishing as described in Steps 5 and 6 to produce the smooth surface required for easy removal of the electroformed foil. Copper-plated brass is recommended for machining mandrels.

Step 2. Machining threads in brass rods with sharp "V" grooves was accomplished by using high-speed tool-steel cutters ground with a chip breaker, or chip groove, as shown in Figure 4. To produce uniformly shaped threads, the tool was used in a direction that is the reverse of that

* Plated in a Dayton Bright Acid Copper Bath, Cu Flex.

normally used for threading rods with such a tool. When the threads were cut by moving the tool in the opposite direction from that shown in Figure 4, the threads were distorted. One side of each thread was almost perpendicular to the axis of the bar, while the other side had nearly the correct angle. This reversal of normal threading technique was required because the threads were cut in one pass. The cutting edges of the tool were polished with 400-grit silicon carbide abrasive paper until a razor-sharp edge was obtained. Final honing of the edges was done on a slowly rotating brass lap with 3-micron diamond-paste abrasives. One tool was used for machining six mandrels and could have been used for additional machining because the cutting edge was still sharp.

Thread cutting was done with a 13-inch Monarch lathe using a cutting feed because thread-cutting gearing would not produce the fine threads needed. Because of this need to use a cutting feed, full thread depths were cut in one pass using a slow rotational speed of under 50 rpm.

Stainless steel was successfully machined using a high-speed threading tool and cutting threads with a 10-mil pitch. Attempts to machine threads finer than 10 mils in stainless steel were not successful. The first reusable mandrel was made by electropolishing a threaded 304 stainless steel rod of 2-inch diameter and 15-inch length. This mandrel was used to electroform the corrugated foils for the first honeycomb structure. Because a useful mandrel was successfully produced from stainless steel, a replacement mandrel from brass was not necessary. The procedure for fabricating a mandrel from brass was developed after the one good stainless steel mandrel was produced.

Step 3. To inspect the thread profile, a replica of the threads was made with a silicone rubber,* sections of which were cut with a sharp knife and examined microscopically. When the replicas showed uniform thread angles and the depths of the grooves were at least 0.6 times the thread pitch, the mandrel was satisfactory. If the threads were not uniform with the required depth, the mandrel was remachined and threads were recut by

* RTV-30 General Electric Co., catalyzed with Catalyst T-9, M&T Chemical, Inc.

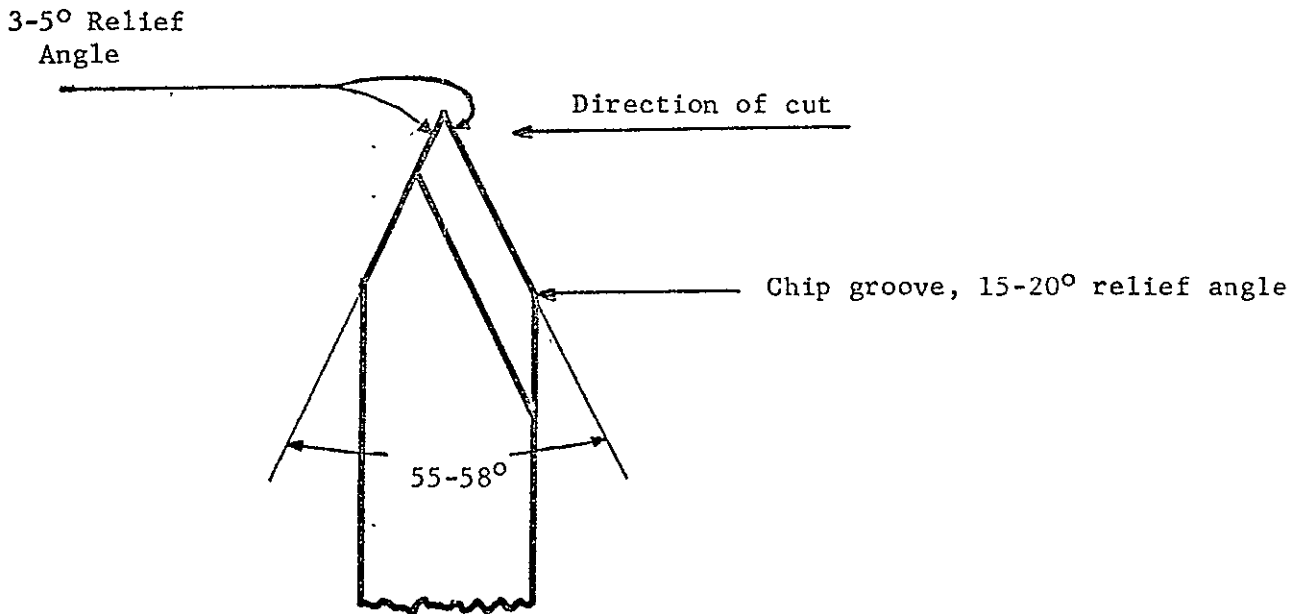


FIGURE 4. CUTTING TOOL USED FOR THREADING MANDRELS

repeating Steps 1 and 2. The RTV silicone rubber allowed a quick inspection to be made before removing the mandrel from the lathe.

Step 4. A smooth file was used to produce a flat side on the mandrel about 1/4 to 3/8 inch wide. The purpose of the flat strip was to provide a starting edge for removing the electroformed foils from the mandrel. Any scratches produced by filing were removed with fine (400-grit) abrasive paper.

Step 5. The machined mandrel had small burrs on the top of each thread. These were removed with abrasive paper (600-grit) while rotating the mandrel on a lathe. Only light pressure was used in order to prevent distortion of the tops of the threads. Abrasion was continued until the burrs appeared by examination at 120X to be removed.

Step 6. Polishing the threads after Step 5 was a very important step. Any nicks or pits remaining in the sides of the threads acted as locks to prevent easy removal of the electroformed foils. To accomplish this polishing, a brush with pointed 3-mil brass wires was held lightly against the rotating mandrel. Three water suspensions of 1.0, 0.5, and 0.05-micron alumina were used in succession to polish the threads. The mandrel was rotated in both directions to insure polishing of both sides of the threads. A rotational speed of 1000 rpm was used. Care was needed to maintain a dilute slurry of abrasive material on the brush. If too little water was used, the alumina packed on the brush acted like a solid abrasive block and cut the tops of the threads. The brass brush was dipped for a few seconds in 300 g/l nitric acid solution to point the ends of the wires.

Step 7. Cleaning to remove the polishing residue from the threads was accomplished by first brushing the mandrel with a dry pointed-wire brass brush, then using a commercial electrolytic cleaner commonly used for electrocleaning. A microscopic examination of the threaded mandrel at 120X was made to determine if polishing had removed most surface defects. When the mandrel was judged smooth enough, the next step was initiated.

Step 8. The mandrel was cleaned for electroplating using conventional techniques and was plated with 0.3 mil of bright nickel* and then about 0.5 to 1.0 mil of bright chromium** using a mixed sulfate-fluosilicate catalyzed chromic acid bath. These plating steps also were done using conventional plating techniques. The purposes of plating were (1) to improve the smoothness of the mandrel with the bright nickel plating and (2) to provide a hard chromium surface. Chromium is an ideal electroforming surface

* Harshaw Perglow Bright Nickel Bath.

** Chromic acid, 250 g/l; sulfuric acid, 2.2 g/l; fluosilicic acid, 7.5 g/l; operated at 120 - 125 F.

because nickel electroplates will not adhere to chromium, so they can be removed easily.

Step 9. Application of the pressure-sensitive tape was a convenient method for masking areas where deposit was undesirable. This masking included a strip on the flattened side of the mandrel.

Step 10. Cleaning of the chromium surface to remove fingerprints and other dirt was done with a fiber bristle brush and magnesium oxide-water slurry. Electrolytic cleaning was not used because the hot alkaline solution would have removed the masking material.

Alternate Mandrel-Fabrication Methods. Two other methods were investigated for fabricating mandrels. The first used a threaded polypropylene rod, which was metallized with silver. Then a nickel shell was electroformed on the plastic by methods similar to the techniques used in the phonograph record industry.⁽²⁾ The polypropylene could be machined with smaller and smoother threads than the brass rods. The electroformed shell was removed from its cylindrical mandrel, straightened, and used as a flat, corrugated electroforming mandrel.

An improvement in the above method for using plastic starting material was devised to insure faithful reproduction of the smooth thread surface. This improvement included metallizing the plastic with silver, copper plating, removing the shell, nickel plating on the threaded side, and chemically dissolving the copper and the silver. The advantage of this improved sequence is that the threaded surface was reproduced directly. In contrast, if the nickel was applied to the chemically deposited silver, the nickel would reproduce any roughness or distortions introduced during the silvering.

The second alternate method considered was that of rolling threads into the mandrel surface. Textured inking rolls are available in the graphic

References are listed on the last page of this report.

arts industry* which have grooves with 5-mil pitches or larger. This method would probably require some refinement to produce grooves less than 5 mils wide. Surface roughness of the grooves in textured rolls which were examined was similar to machined threads and would require polishing. An advantage of rolling techniques is that large-diameter drums can probably be made for electroforming corrugated nickel foil by a continuous process.

Corrugated-Foil Electroforming. After the brass mandrels were prepared as described in the section "Electroforming Mandrel Fabrication", the mandrels were placed in a sulfamate nickel plating bath.** The mandrels were rotated at 7 rpm and plated at 130 F, pH 4.0 ± 0.2 , 60-80 asf, for 4 to 5 minutes to apply 0.3 to 0.4 mil of plate. To remove the foil, the plated mandrel was washed in cold water and the edge of the nickel foil was lifted with a sharp-pointed tool along the flat side of the mandrel. After removal of a foil, the mandrel was replaced in the nickel electroforming bath for electroforming the next foil. Attempts to electroform corrugated foils 0.2 mil thick were inconsistently successful. Smoother threaded mandrels would be required to make foils 0.2 mil thick.

Flat-Foil Electroforming. A similar technique was used for electroforming flat foils, except that a smooth cylindrical mandrel was used. Flat foils about 0.2 mil thick were formed and used for fabricating the honeycomb structure. Electroformed foils as thin as 0.1 mil were made but were considered too difficult to handle by the present techniques used on this program.

Fabricating Plaques. Honeycomb structures as shown in Figures 1, 2, and 3 were made by stacking electroformed foils 2.86 x 5.0 cm in a graphite block. A weight was placed on the top of the block to compress the

* Textured rolls can be obtained from Pamarco, Inc., Roselle, N. J., or Consolidated Engravers, Charlotte, N. C.

** Sulfamate nickel bath, Type SN, obtained from Allied Chemical Company.

foils to a height of 0.32 cm and the assembly was heated to 1940 F for 1 hour in hydrogen. Bonding was adequate with this heating cycle. Based on the examination of these three structures, the configuration shown in Figure 3 was selected as the best structure, and this configuration was used to fabricate a honeycomb block 2.86 x 2.86 x 5.0 cm using the five sizes of corrugated foils.

Slicing of the honeycomb block into 0.075 to 0.10-cm-thick plaques was done by EDM (Electric Discharge Machining) and by grinding. EDM was used to cut several plaques 0.13-cm-thick using a 0.013-cm-diameter wire as the cutting tool. Excellent control of plaque thickness was obtained and no filler was required. However, cutting times were excessive because each cut to produce one plaque required about 7 hours. Because only a single-wire cutting fixture is currently available, the EDM method of slicing the honeycomb was abandoned. Multiple-wire cutting equipment could be set up to make this method feasible for production use.

Slicing by grinding the first set of honeycomb plaques from the honeycomb block was accomplished by filling the structure with Apiezon wax and cutting thin slices with a 0.20-cm-thick grinding wheel. Thickness of slices varied from 0.09 to 0.12 cm because the heat from the friction expanded the wax and metal. After grinding, the slices were abraded with 320-grit silicon carbide paper to remove grinding burrs. An electrolytic etch in 10 percent hydrochloric acid for about 15 seconds at 32 amp/sq cm of plaque area was used for final burr removal. The wax was then dissolved in benzene.

The other four sizes of honeycomb blocks were filled with an epoxy mixture* of Epi-Rez 5077 (67 percent by volume) and Epi-Cure 856 (33 percent by volume) and cured for 48 hours at room temperature before being cut into 2.3-cm-thick slices. The epoxy was far superior to the wax because the thermal stability of the epoxy allowed faster grinding rates.

* Epoxy materials obtained from Celanese Resins Division of Celanese Coatings Company.

After the plaques were sliced from the structure, they were polished to a thickness of 0.20 cm on abrasive paper (600-grit silicon carbide) to remove grinding marks and then were etched electrolytically in 1.2 normal hydrochloric acid to remove polishing burrs. Removal of the epoxy filler was accomplished in 1 to 2 hours in a 500 g/l chromic acid solution heated to 82 to 88 C.

Alloy Honeycomb Structure

Nickel honeycomb structures with a thin cadmium-nickel alloy coating were considered for increasing the receptivity of the metal surface to cadmium metal deposition during charging. Honeycomb plaques were cleaned and electroplated with cadmium metal using a high-throwing-power cyanide bath.* Heating the plaque in a hydrogen atmosphere to melt the cadmium evaporated the metal instead of alloying the nickel and cadmium as expected. Alloy electrodes were not successfully made and this approach was discontinued.

Corrugated Plaques

An experiment was planned and carried out during this program to evaluate an electrode supporting structure, or plaque, consisting of a single sheet of corrugated nickel foil. This experiment was designed to show if a thin coating of cadmium hydroxide in contact with such a nickel sheet would provide a system wherein efficient utilization of cadmium hydroxide could be obtained. The results, described in Task D, Electrochemical Evaluation of Electrodes, showed that at least 70 percent of the cadmium hydroxide can be utilized electrochemically.

An electroformed corrugated foil about 0.0007 cm thick with corrugations 0.013 cm wide was used as a plaque. The corrugated foil provided a lightweight support for the cadmium hydroxide active material. Details of the cell construction and electrochemical cycling program are described in Task D.

* Metal Finishing Guide Book Directory, 1970 Edition, page 254.

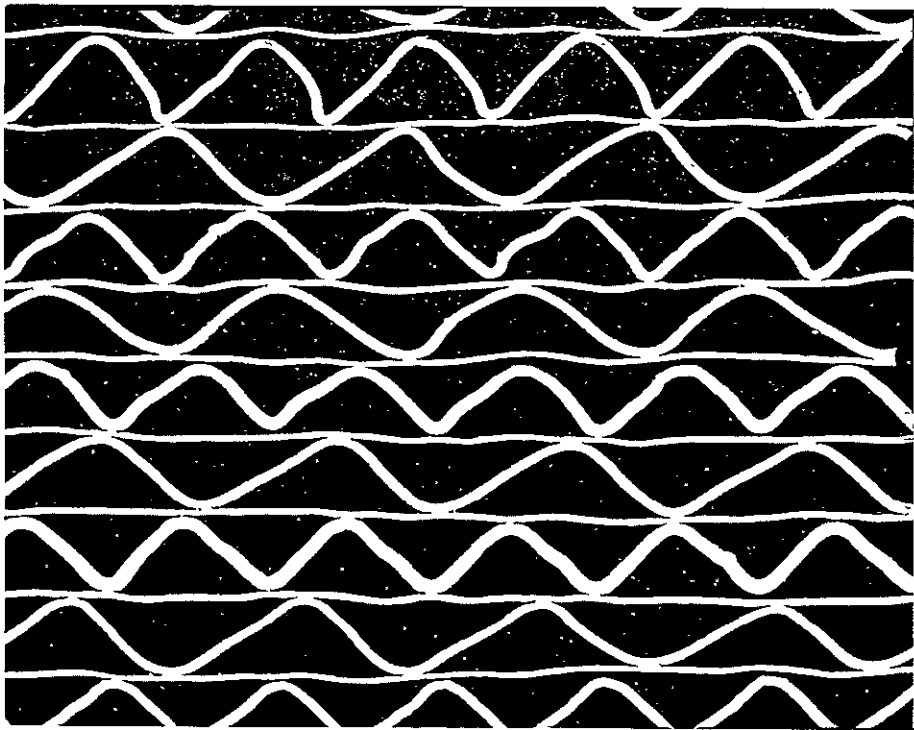
Task B. Plaque Characterization

Pore Size, Shape, and Internal Area. Honeycomb plaques were made 2.86 cm (1-1/8 inch) square and 0.084 ± 0.005 cm (33 ± 2 mils) thick. The edges were coined to leave a porous area 2.54 cm (1 inch) square. Plaque characteristics were computed and the resulting values of the five sizes of honeycomb plaques are given in Table 1. Figures 5, 6, 7, 8, and 9 show cross sections of typical honeycomb plaques at 100X. The plaques were filled with epoxy and polished by metallographic techniques before pictures were taken.

Flexibility of Plaques. The flexibility of unimpregnated plaque material was measured by bending the plaques tightly around glass rods having diameters from 0.32 to 2.2 cm. The honeycomb plaques were bent in two directions at right angles to each other, that is, parallel and perpendicular to corrugations of nickel sheets. All of the honeycomb plaques could be bent around any of the rods in either direction without the bonds between nickel sheets being broken. This resistance to breaking, even when severely bent, shows that the honeycomb plaques have a high degree of structural integrity and that the bonding of the stacked foils was complete throughout the block of stacked foils.

When a sintered-powder plaque was bent, the sintered powder cracked in the direction parallel with the bend. The sintered powder did not break away from the plaque, which indicates that it was properly bonded through the expanded nickel substrate.

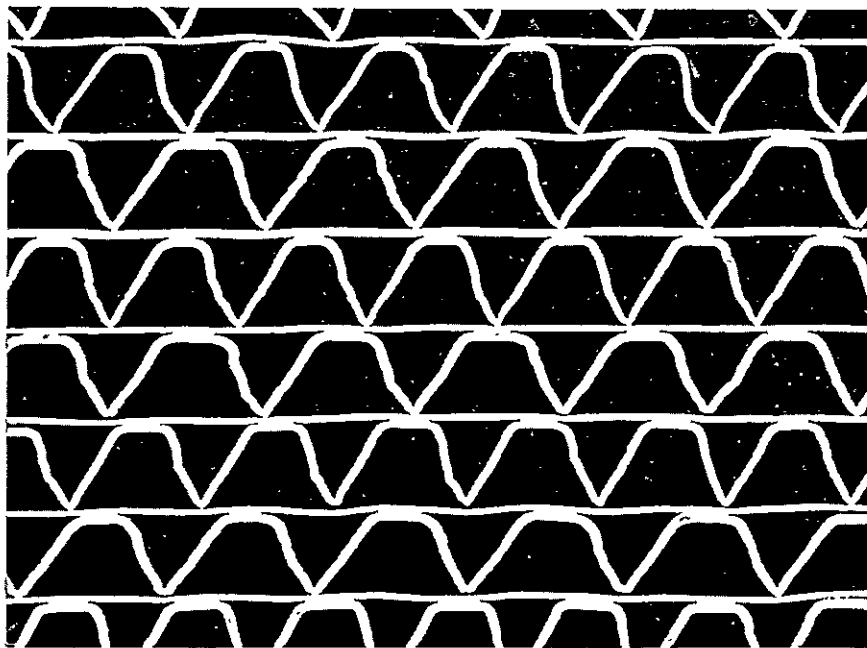
Electrical Resistance. Electrical-resistance measurements were made both perpendicular to and parallel with the direction of the foils in the plaques. The measurements are given in Table 2, which shows the electrical resistances of the honeycombs to be about 1/3 larger to 1/2 smaller than resistivities measured for sintered-powder plaques.



100X

8E 664

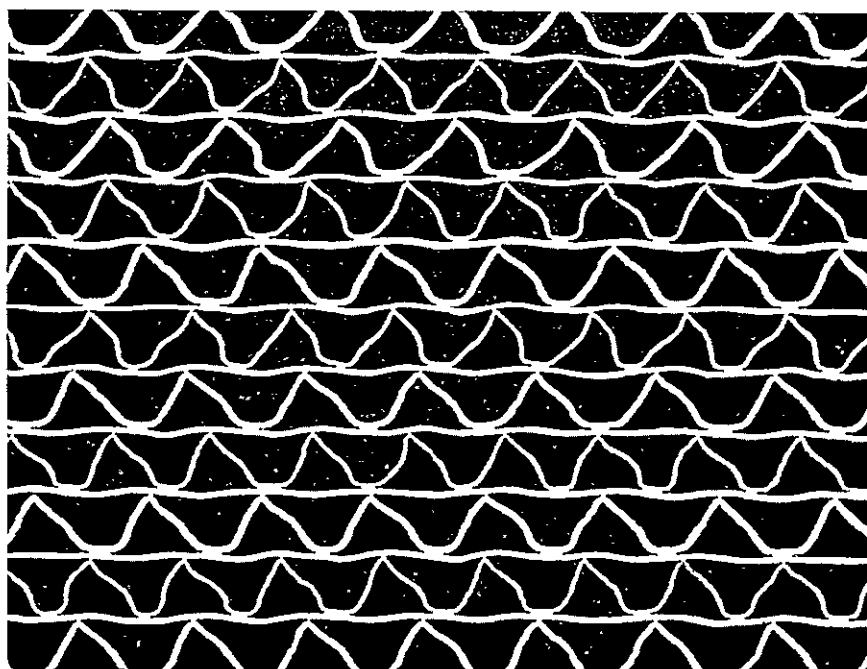
FIGURE 5. PHOTOMICROGRAPH OF HONEYCOMB PLAQUE WITH 0.015 CM PORES



100X

1F 337

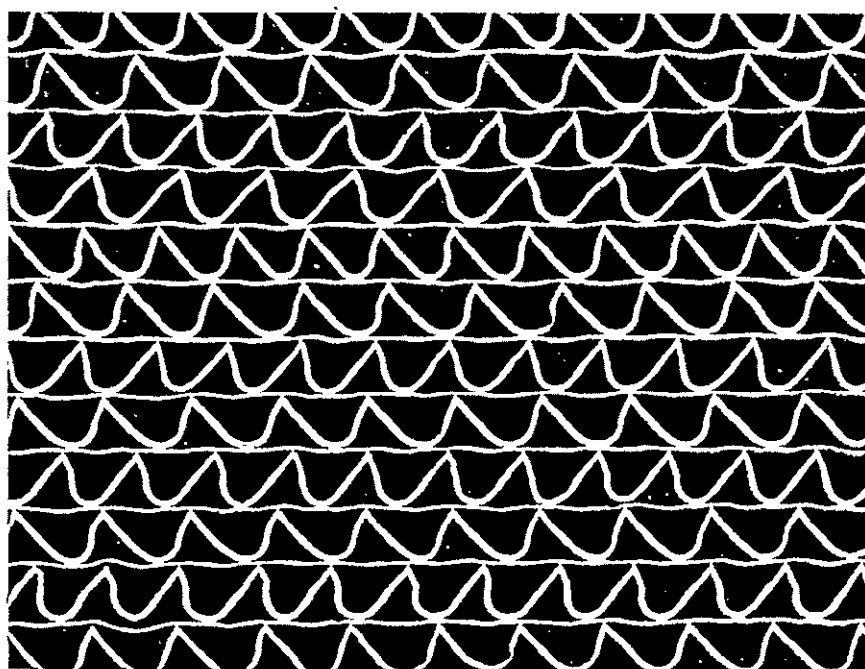
FIGURE 6. PHOTOMICROGRAPH OF HONEYCOMB PLAQUE WITH 0.01 CM PORES



100X

1F 336

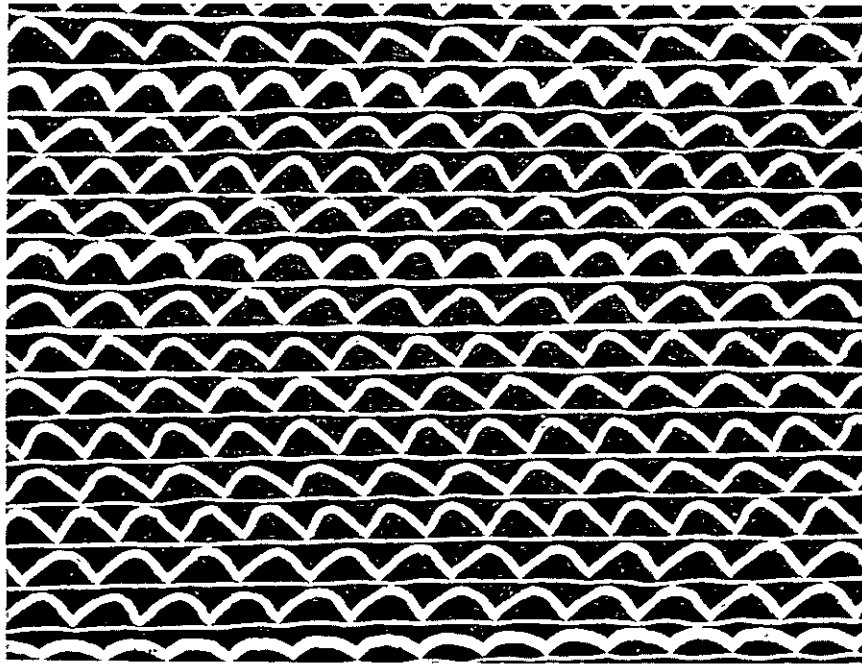
FIGURE 7. PHOTOMICROGRAPH OF HONEYCOMB PLAQUE WITH 0.0076 CM PORES



100X

1F 335

FIGURE 8. PHOTOMICROGRAPH OF HONEYCOMB PLAQUE WITH 0.0061 CM PORES



100X

1F 334

FIGURE 9. HONEYCOMB PLAQUE WITH 0.0049 CM PORES

TABLE 1. PHYSICAL CHARACTERISTICS OF HONEYCOMB PLAQUES

Corrugation Width, cm	Porosity, percent	Internal Surface Area		Pore Size, cm ^(c)	Foil Thickness, cm	
		cm ² /g ^(a)	cm ² /g ^(b)		Flat	Corrugated
0.025	82	204	384	0.0153	0.0008	0.0013
0.018	86	231	306	0.0107	0.0009	0.0010
0.013	76	305	367	0.0076	0.0007	0.0007
0.010	77	305	371	0.0061	0.0006	0.0008
0.008	66	246	381	0.0049	0.0006	0.0011
Powder plaques	80	880 ^(d)	--	0.0015 ^(d)	--	--

(a) Internal area was calculated from foil thickness and length measured from cross sections of plaques as shown in Figures 5, 6, 7, 8, and 9.

(b) Internal area was calculated from measuring weight and thickness of corrugated foil and assuming the corrugated foils had sharp corners and all angles were 60 degrees. The difference between the two values resulted from rounded corners and shrinkage during heat bonding.

(c) Pore size calculated as inscribed circle in triangular-shaped pore.

(d) Measurements of pore size and internal surface area were not made. However, reported data (NASA CR-54831) are included for comparison.

TABLE 2. ELECTRICAL RESISTANCE OF PLAQUES

Plaque Type	Resistance, microohms	
	Perpendicular to Foils	Parallel With Foils
Sintered powder	2.5 - 2.8	2.5 - 2.8
0.015-cm Honeycomb	3.3	Not measured
0.010-cm Ditto	2.4	3.3
0.0076-cm "	2.1	2.8
0.0061-cm "	" 1.35	1.7
0.0049-cm "	1.3	1.5

Task C. Plaque Impregnation

Honeycomb Plaque

After the porous-plaque structures were prepared and characterized as described under Tasks A and B, respectively, they were coined to leave a porous area of 2.54 x 2.54 cm. A 0.0254-cm-thick nickel-foil tab was spot welded to one edge of the electrode as shown in Figure 10.

The technique chosen for this work was standard vacuum impregnation with aqueous cadmium nitrate solution followed by cathodization in hot KOH. This method was chosen because it is used throughout the battery industry to make cadmium electrodes for sintered-plate nickel-cadmium batteries. It also meets the requirements of NASA Specification No. S-716-P-23. Minor variations of a proprietary nature may exist in the process from one manufacturer to another, but the basic process seems to be similar in all known cases. By using this standard vacuum-impregnation process, it was expected that the electrodes having the new plaque structures could be compared readily with commercial electrodes since the method of

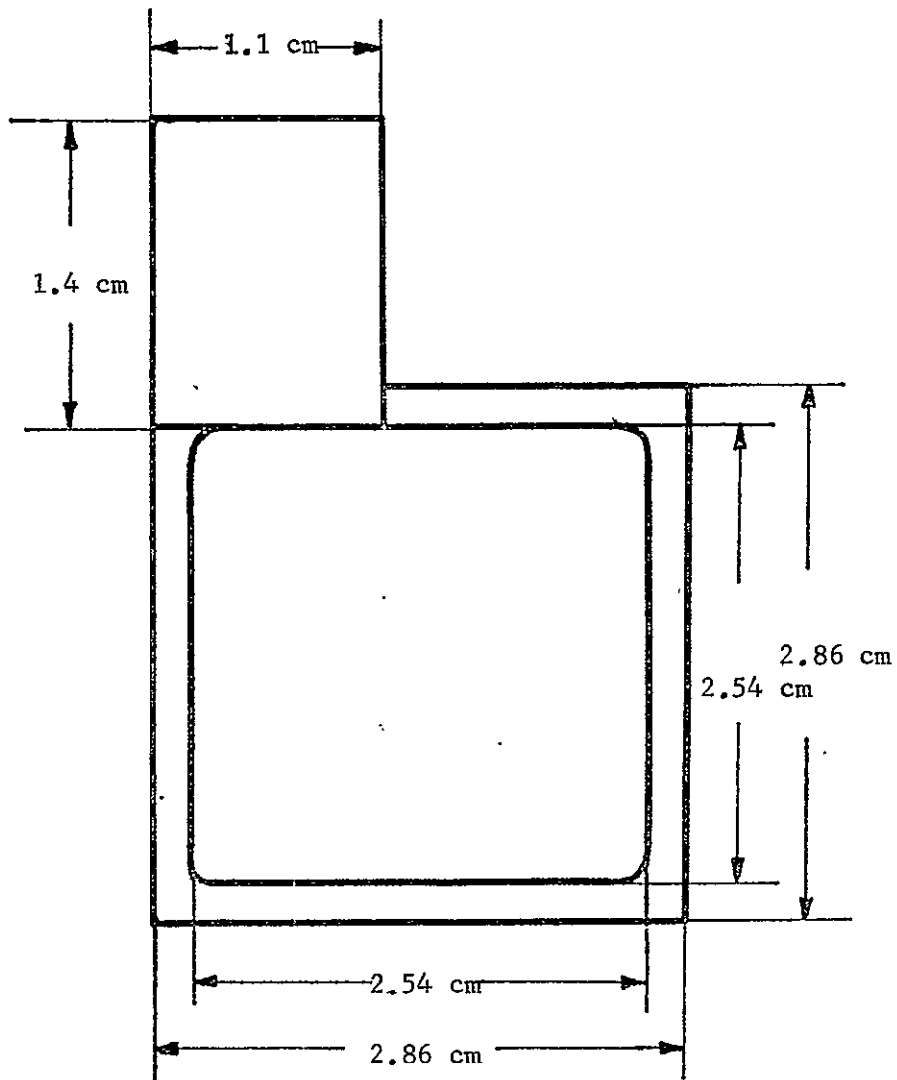


FIGURE 10. PLAQUE WITH COINED EDGE AND TAB ATTACHED BY SPOT WELDING

impregnation was the same for both types of electrodes. Later results showed that this impregnation method was not optimum for the honeycomb plaques.

Description of the Impregnation Process. The basic vacuum-impregnation process has been described many times in the literature, e.g., References (1), (3), and (4). The specific details of the process as used in this work are as follows:

- (1) Soak the plaques for 5 minutes under vacuum and for an additional 5 minutes under atmospheric pressure in a cadmium nitrate solution prepared in the following manner: Dissolve 1360 g of $\text{Cd}(\text{NO}_3)_2 \cdot 4\text{H}_2\text{O}$ in enough warm distilled water to make 1 liter of solution. Add 1 g/l of polyethylene glycol MW 6000. After the polyethylene glycol is dissolved, vacuum filter through a fine filter paper such as Whatman No. 5 to remove any dirt from the solution. Add concentrated nitric acid to adjust the free-acid concentration to the desired value of 3-4 g/l.
- (2) Cathodize the plaques containing the cadmium nitrate solution for 20 minutes in 20 weight percent KOH which has been preheated to 90-100 C. The current density is 6.4 ampere per square cm of plaque. The plaques are placed in the electrolyte with the current flowing as described in References (1), (3), and (4).
- (3) Rinse the cathodized plates in distilled water and scrub gently with a nylon bristled brush to remove $\text{Cd}(\text{OH})_2$ precipitated on the surface. Wash the plates in distilled water at 40 C for 4 hours or until the last drop of wash water from a plate shows no KOH when tested with phenolphthalein indicator.
- (4) Dry the plates at 60 C. This drying is preferably done in a vacuum oven to prevent the impregnated plates from absorbing CO_2 .

These four steps are referred to as an impregnation cycle. In order to obtain the desired capacity for an electrode, it is necessary to perform between four and eight impregnation cycles.

Description of Apparatus. Vacuum Impregnation Chamber. The apparatus used to impregnate plaques with cadmium nitrate solution is shown in Figure 11. It consists of a bell jar placed over a Lucite tank containing the plaques to be impregnated. The bell jar is connected through Tygon tubing to a reservoir of the impregnating solution and to a vacuum pump. The pressure should be about 10 mm Hg before impregnation is begun. The solution is transferred from the reservoir to the impregnation tank by raising and tilting the reservoir. The Lucite tank was grooved to hold the plaques in an upright position without their touching each other. Ten plaques were impregnated at one time using this equipment.

Polarization Equipment. A photograph of the polarization tank is shown in Figure 12. The tank was made of nickel and served as the counterelectrode during cathodization. The plaques to be cathodized were individually held in nickel-plated battery clips connected to a nickel bus bar. The bus bar rests on a Lucite insulator on top of the nickel tank. Ten plaques were processed simultaneously in this tank. After the plaques impregnated with cadmium nitrate were placed in the clips and lowered into the tank, the negative terminal of a constant-current power supply was connected to the bus bar and the positive terminal was connected to the nickel tank. The power supply was turned on and 20 percent KOH that had been previously heated to 90-100 C in a stainless steel beaker was poured into the tank to complete the circuit. Electrolysis was performed for 20 minutes at a current density of 0.4 amp per square cm of electrode.

Electrode Wash Tank. After the electrodes were removed from the cathodization tank, rinsed with distilled water, and scrubbed with a nylon brush to remove precipitated $\text{Cd}(\text{OH})_2$ from their surfaces, they were washed for 4 hours in distilled water at about 40 C. The distilled water had a

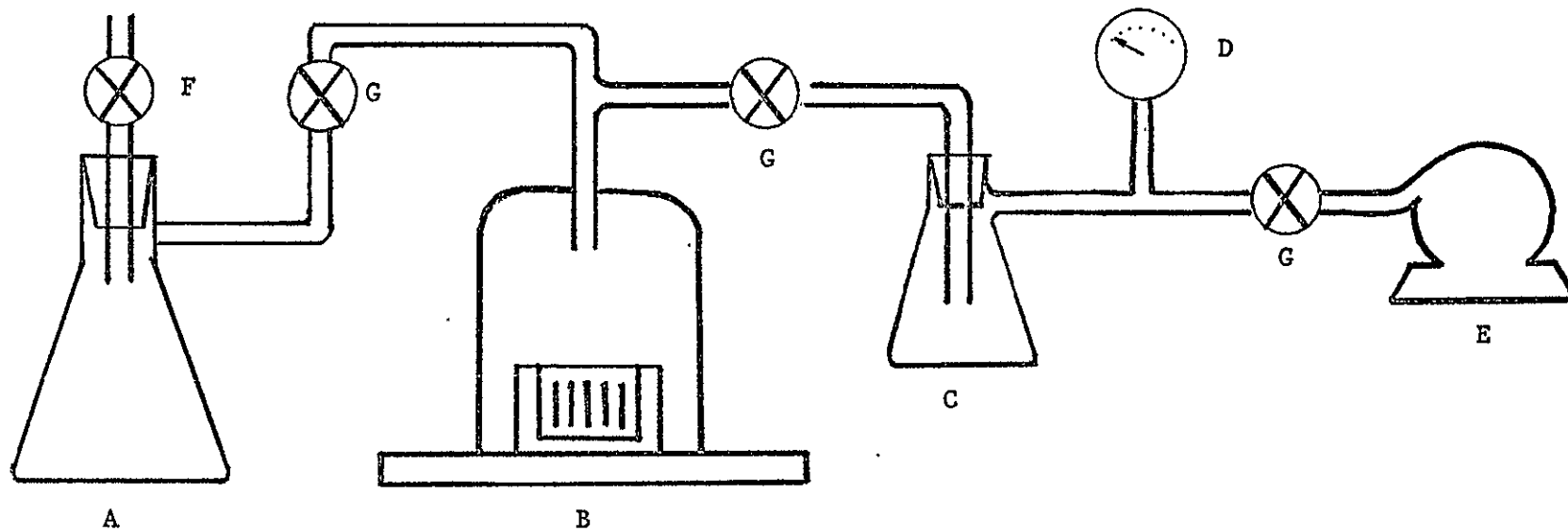


FIGURE 11. VACUUM IMPREGNATION APPARATUS

- A Solution reservoir, 500-ml flask
- B Bell jar over impregnation tank containing plaques
- C Trap
- D Gauge
- E Vacuum pump
- F Air inlet
- G Tubing clamps

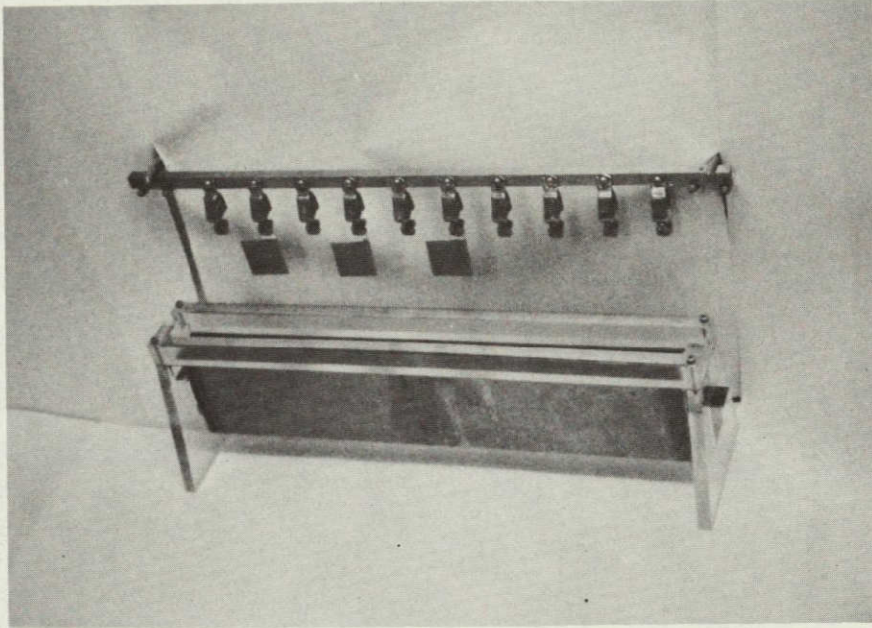


FIGURE 12. POLARIZATION TANK

specific resistance over 500,000 ohm-cm. The wash tank used in this work was a covered polyethylene pan. A recirculating pump was connected through Tygon tubing to inlet and outlet holes cut in the pan. The wash water was continuously circulated about the electrodes, which were held in a stainless steel wire basket. The wash water was replaced about every 30 minutes during the 4-hour washing time.

After washing, the electrodes were dried overnight in a vacuum oven at 60 C.

Impregnation Results. Twenty honeycomb plaques of each set with 0.01, 0.0076, 0.0061, and 0.0049-cm pore diameters, 10 honeycomb plaques with 0.015-cm pore diameters, and 20 sintered-powder plaques were impregnated with cadmium hydroxide using the standard vacuum-impregnation procedure. (7) It was decided in advance, as part of the experimental plan, that all plaques would receive as many impregnation cycles as were required to fill approximately 40 percent of the pore volume with cadmium hydroxide. In order to determine when the plaques were filled with the desired amount of cadmium hydroxide, the partially impregnated plaques were dried and weighed after each impregnation cycle. The assumption was made that the weight gain was due entirely to cadmium hydroxide, and impregnation was continued until the weight of cadmium hydroxide calculated to fill 40 percent of the pore volume was reached. Table 3 shows that more impregnation cycles were required to reach the same calculated percent of pore volume filled for honeycomb plaques than for sintered-powder plaques.

Subsequent chemical analysis of the impregnated electrodes showed that the starting assumption that all the weight gain during impregnation was due to cadmium hydroxide was invalid. The honeycomb electrodes were found to contain a smaller ratio of cadmium hydroxide to metallic cadmium than did the sintered-powder electrodes. Total cadmium was determined by titrating with EDTA aliquot solutions of the electrodes dissolved in nitric acid using the procedure given on pages 7 and 8 of Reference (6). Then, the amount of metallic cadmium in the impregnated material was calculated from the difference between the weight gain after the final impregnation

TABLE 3. CYCLES REQUIRED TO IMPREGNATE ^(a) HONEYCOMB PLAQUES

Pore Size, cm	Cycles for First Batch	Cycles for Second Batch	Calculated Percent Volume Filled of First Batch	Calculated Percent Volume Filled of Second Batch
0.015	8	(b)	36	(b)
0.010	10	11	39.4	35.7
0.0076	10	14	39.3	38.7
0.0061	9	10	38.6	37.7
0.0049	9	10	43.9	40.8
Powder plaques	4	4	39.5	39.7

(a) Impregnation was done using ten plaques in a batch.

(b) Only one batch of ten plaques was used.

cycle and the chemical analysis data for total cadmium using Equation (3) below. In this calculation, the total weight gain is assumed to be due only to metallic cadmium and cadmium hydroxide. That is, any small amount of cadmium oxide is assumed to be negligible. Also, corrosion of the nickel plaque by the cadmium nitrate impregnating solution considered to be negligible because (1) the polyethylene glycol in the impregnating solution acts as a corrosion inhibitor, and (2) the solution was still almost colorless after impregnation. Even a small amount of nickel dissolved in the cadmium nitrate solution would have given it a definite green color. With these assumptions and facts in mind:

$$\text{Observed wt gain} = \text{wt Cd} + \text{wt Cd(OH)}_2, \text{ and} \quad (1)$$

$$\text{Analyzed total Cd} = \text{wt Cd} + \frac{112.4}{146.4} \text{wt Cd(OH)}_2 \quad . \quad (2)$$

Solving Equations (1) and (2) for wt Cd gives

$$\text{wt Cd} = \frac{\text{total Cd} - \frac{112.4}{146.4} \text{wt gain}}{1 - \frac{112.4}{146.4}} \quad . \quad (3)$$

Moreover, if the total cadmium were present only as cadmium hydroxide, the theoretical weight gain as Cd(OH)_2 is given by

$$\text{theoretical wt gain as Cd(OH)}_2 = \frac{146.4}{112.4} \text{total Cd} \quad (4)$$

The theoretical wt gain as Cd(OH)_2 was calculated from the chemical analysis data for total Cd using Equation (4). Table 4 shows the actual weight gain, the calculated theoretical amount of cadmium hydroxide, Equation (4), and the calculated amount of metallic cadmium, Equation (2), for a representative sample of each type of electrode.

TABLE 4. ANALYSIS OF CADMIUM ELECTRODES

Electrode	Theoretical Cd(OH) ₂ , g	Actual Gain, g	Cd, g
Sintered powder	0.845	0.800	0.149
0.015-cm Honeycomb	0.902	0.801	0.334
0.010-cm Ditto	1.140	0.932	0.688
0.0076-cm "	0.980	0.860	0.397
0.0061-cm "	1.090	0.908	0.602
0.0049-cm "	0.890	0.695	0.297

The data in Table 4 show that all electrodes actually contained more cadmium than was desired. The percent of the pore volume of each plaque which would be filled with Cd(OH)₂ if all cadmium were in this form is given in Table 5.

TABLE 5. CALCULATED AMOUNT OF PLAQUE PORE VOLUMES FILLED WITH Cd(OH)₂

Electrode	Plaque Pore Volume, cm ³	Theoretical Cd(OH) ₂ Volume, cm ³	Pore Volume If Filled With Cd(OH) ₂ , Percent
Sintered powder	0.412	0.177	43.0
0.015-cm Honeycomb	0.428	0.189	44.0
0.010-cm Ditto	0.398	0.238	59.8
0.0076-cm "	0.467	0.205	43.8
0.0061-cm "	0.359	0.228	63.5
0.0049-cm "	0.328	0.186	56.6

Figure 13 shows a magnified surface view of an impregnated honey-comb plaque (black) which contains a mixture of metallic cadmium (dark gray) and cadmium hydroxide (white).

Electrode Formation. After the electrodes were impregnated to what was thought to be about 40 percent of the pore volume with $\text{Cd}(\text{OH})_2$, they were given a series of formation cycles. These cycles are reported to serve two functions⁽⁷⁾: (1) impurities such as nitrate and carbonate and loosely adhering particles are removed from the electrodes and (2) the active material is "exercised" by the series of charge-discharge cycles which probably increases the lattice defects and the surface area of the active material.

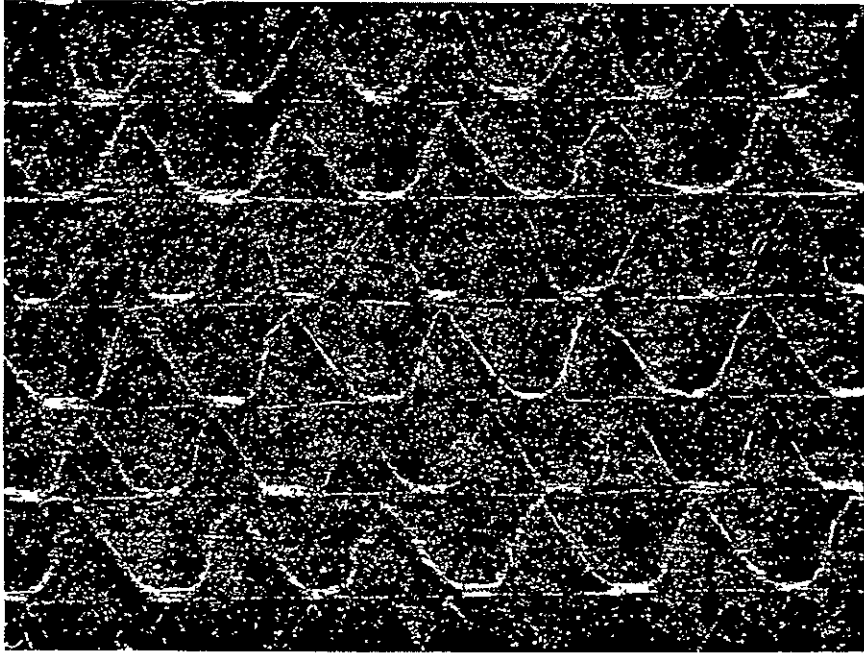
To implement the desired formation the cadmium electrodes were arranged alternately between nickel hydroxide positive electrodes with two layers of perforated polypropylene separators between adjacent electrodes. The electrodes were connected so that all cadmium electrodes were in parallel, as were all nickel electrodes. Each formation cell contained four cadmium electrodes and five nickel electrodes. The electrolyte in the formation cells was 30 percent KOH. The electrodes were soaked in the electrolyte for 16 to 24 hours before cycling was begun. The series of formation cycles was performed as follows:

Cycle 1. Charge for 16 hours (overnight) at the C/7 rate based on the theoretical capacity of the negative electrodes. This theoretical capacity was calculated from the total weight gain during impregnation assuming it to be in the form of $\text{Cd}(\text{OH})_2$. Discharge at the C/7 rate to 1 volt per cell.

Cycle 2. Same as Cycle 1.

Cycle 3. Charge at C/5 for 7 hours. Discharge at C/5 until both sets of electrodes are completely discharged.

Following the third formation cycle, the electrodes were rinsed in distilled water, wet brushed to remove any loose particles, and washed for 4 hours in



100X

1F 338

FIGURE 13. PHOTOMICROGRAPH OF HONEYCOMB PLAQUE
AFTER EIGHT IMPREGNATIONS

NOT REPRODUCIBLE

distilled water at 40 C as was done during impregnation. They were then stacked between layers of filter paper and dried at 60 C. The stacks of electrodes were clamped between pieces of Lucite to prevent possible warping during drying.

Corrugated Plaque

To evaluate the concept of a thin corrugated foil as a plaque, a single corrugated foil with 0.013-cm-wide corrugations was coated with powdered cadmium hydroxide and assembled into a two electrode cell for cycling. Cycling data are given in the following (Task D) section of this report.

Cadmium hydroxide powder was made by reacting a cadmium nitrate solution with an excess of potassium hydroxide solution to precipitate cadmium hydroxide. The product was filtered, washed with distilled water, dried at 95 C, and ground into a fine powder. The corrugated foil was covered with a layer of this powder after the foil was cleaned and electroplated with about 0.0075 cm of cadmium metal. The plating step was used to show that all dirt and oxides had been removed from the nickel foil.

Task D. Electrochemical Evaluation of Electrodes

Electrode-Capacity Measurements. Before any cycling experiments were conducted, capacities of single cadmium electrodes were measured by immersing one electrode in a beaker of 30 percent potassium hydroxide solution. Each electrode was cycled using two nickel-foil counterelectrodes. The approximate capacities were determined so that charge and discharge currents based on C rates could be selected. The C rate is the current which will deliver the specified ampere-hour capacity in 1 hour. The capacity of the sintered-powder electrodes estimated from formation cycling data was 240 mA-hr. When a single sintered-powder electrode was discharged at 240 mA it ran for 70 minutes before the knee of its discharge curve with respect to Hg/HgO reference electrode was reached. Therefore, it had

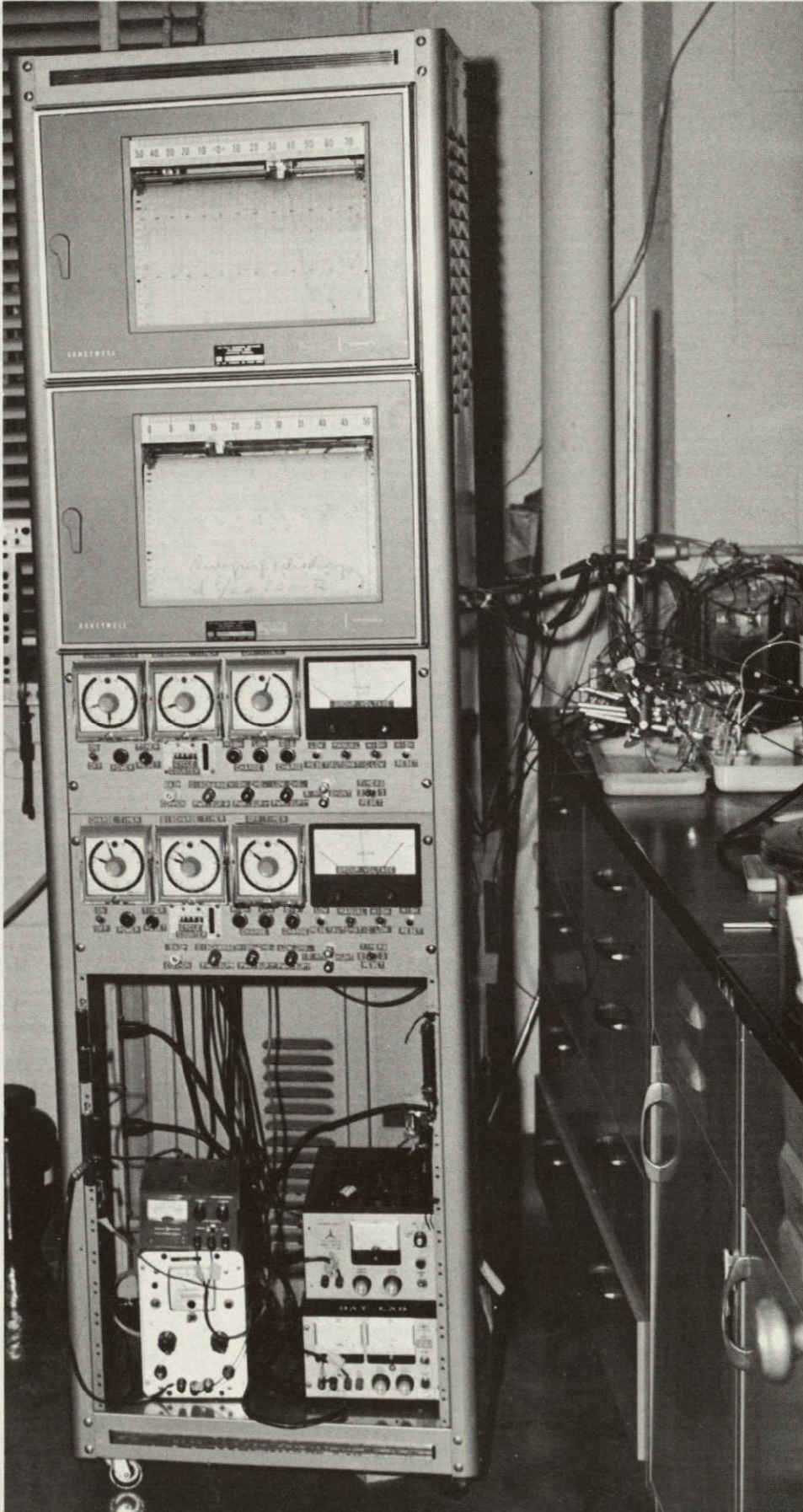
a capacity of 280 mA-hr and the C rate used for the sintered-powder electrodes was 280 mA. When the 0.0061 and 0.0076-cm honeycomb electrodes were discharged at 240 mA, they ran for 30 minutes. Thus, their C rate was 120 mA. This same rate was also used for the other three pore sizes of honeycomb electrodes with the expectation that this would allow direct comparison of pore sizes.

Electrode Performance During Cycling. A group of honeycomb electrodes of each size and a group of sintered-powder electrodes were cycled according to the following cycle regimes:

<u>Cycle Regime</u>	<u>Charge Rate</u>	<u>Discharge Rate</u>
1	C/2	C
2	C/2	C/2
3	C	C
4	2C	2C
5	C/4	C/4
6	4C	4C

Each group received a minimum of five charge-discharge cycles at each regime. Cycling was performed using the automatic cycling facility shown in Figure 14. Each electrode was operated in a separate cell. The cells consisted of one negative and two positive electrodes. One layer of Pellon 2505 was used as the separator. Two Plexiglas end plates held each cell together with stainless steel bolts. Cells were placed in an open beaker filled with 30 percent potassium hydroxide. The potential of the cadmium electrodes during charge and discharge was measured with respect to a Hg/HgO reference in the same solution.

Table 6 shows the capacity in ampere-hours at different charge and discharge rates of one sintered powder and five different honeycomb electrodes. These capacities obtained from the potential time curves represent a medium value of the ten electrodes which were cycled simultaneously.



NOT REPRODUCIBLE

FIGURE 14. AUTOMATIC CYCLING FACILITY

TABLE 6. CAPACITY OF CADMIUM ELECTRODES
DURING CYCLING EXPERIMENTS

Charge Rate	Hydrogen-free Capacity Amp-hr	Discharge Rate	Discharge Capacity Amp-hr
<u>Sintered-Powder Electrode</u>			
140	0.270	280	0.219
140	0.231	140	0.112
280	0.168	280	0.163
560	0.121	560	0.121
70	0.199	70	0.008
1120	0.149	1120	0.103
<u>Honeycomb Electrode With 0.015 cm Pore Diameter</u>			
60	0.177	120	0.176
60	0.195	60	0.193
120	0.191	120	0.176
240	0.188	240	0.178
30	0.216	30	0.216
480	0.124	480	0.122
<u>Honeycomb Electrode With 0.0107 cm Pore Diameter</u>			
60	0.270	120	0.240
60	0.245	60	0.160
120	0.238	120	0.218
240	0.200	240	0.196
30	0.320	30	0.296
480	0.172	480	0.164
<u>Honeycomb Electrode With 0.0076 cm Pore Diameter</u>			
60	0.147	120	0.142
60	0.242	60	0.237
120	0.164	120	0.158
240	0.136	240	0.128
30	0.220	30	0.207
480	0.160	480	0.144

TABLE 6. (Continued)

Charge Rate mA	Hydrogen-free Capacity Amp-hr	Discharge Rate mA	Discharge Capacity Amp-hr
<u>Honeycomb Electrode With 0.0061 cm Pore Diameter</u>			
60	0.263	120	0.210
60	0.197	60	0.178
120	0.166	120	0.146
240	0.148	240	0.136
30	0.276	30	0.270
480	0.140	480	0.128
<u>Honeycomb Electrode With 0.0049 cm Pore Diameter</u>			
60	0.114	120	0.108
60	0.125	60	0.120
120	0.118	120	0.112
240	0.084	240	0.076
30	0.142	30	0.142
480	0.072	480	0.072

The sintered-powder electrodes showed a large amount of cadmium migration compared with the honeycomb electrodes. Enough cadmium evidently migrated into the separator to short the cells. The loss of capacity due to a short is clearly seen in Table 6 at the 70-mA discharge. The increase in capacity at the subsequent 1120-mA rate is probably due to breaking the short during the high-rate charge. The honeycomb electrodes did not show any significant loss of cadmium into the separator. As seen in Table 6, the honeycomb structures maintained their capacity throughout the cycling regimes much better than did the sintered-powder electrodes. During each of the minimum of five charge-discharge cycles at each regime, the honeycomb electrodes showed a trend of increasing capacity from cycle to cycle. This increasing capacity is a reasonable observation, because the electrodes contained an excess of cadmium metal, as was shown in Table 4. During each discharge some of the metal is oxidized and converted to active cadmium hydroxide.

Most of the honeycomb electrodes exhibited a decrease both in hydrogen-free charge and in discharge capacity as charge and discharge currents were increased. It is well known that battery capacities decrease with increasing currents and that this behavior can be explained as caused by increased polarization at higher current densities. Notice in Table 6, however, that some of the discharge capacities at 60 mA for the same honeycomb differ from the discharge capacities at 60 mA for the same honeycomb structures. This implies that the honeycomb structures might be capable of higher rate discharges than the presently used sintered-powder electrodes.

The capacities listed in Table 6 have an uncertainty of 10 to 15 percent associated with them because of the time required by the multipoint recorder to make two consecutive measurements of the potential of the same cell. The variation of capacity among ten electrodes within a group at any given current for five cycles was less than the experimental uncertainty associated with the recorder.

Figure 15 shows charge and discharge curves for a sintered-powder electrode at 280 mA and curves for a 0.0107-cm-pore-diameter honeycomb electrode at 240 mA for comparison. Both types of electrode have the same

Electrode Potential, mv vs Hg/HgO reference

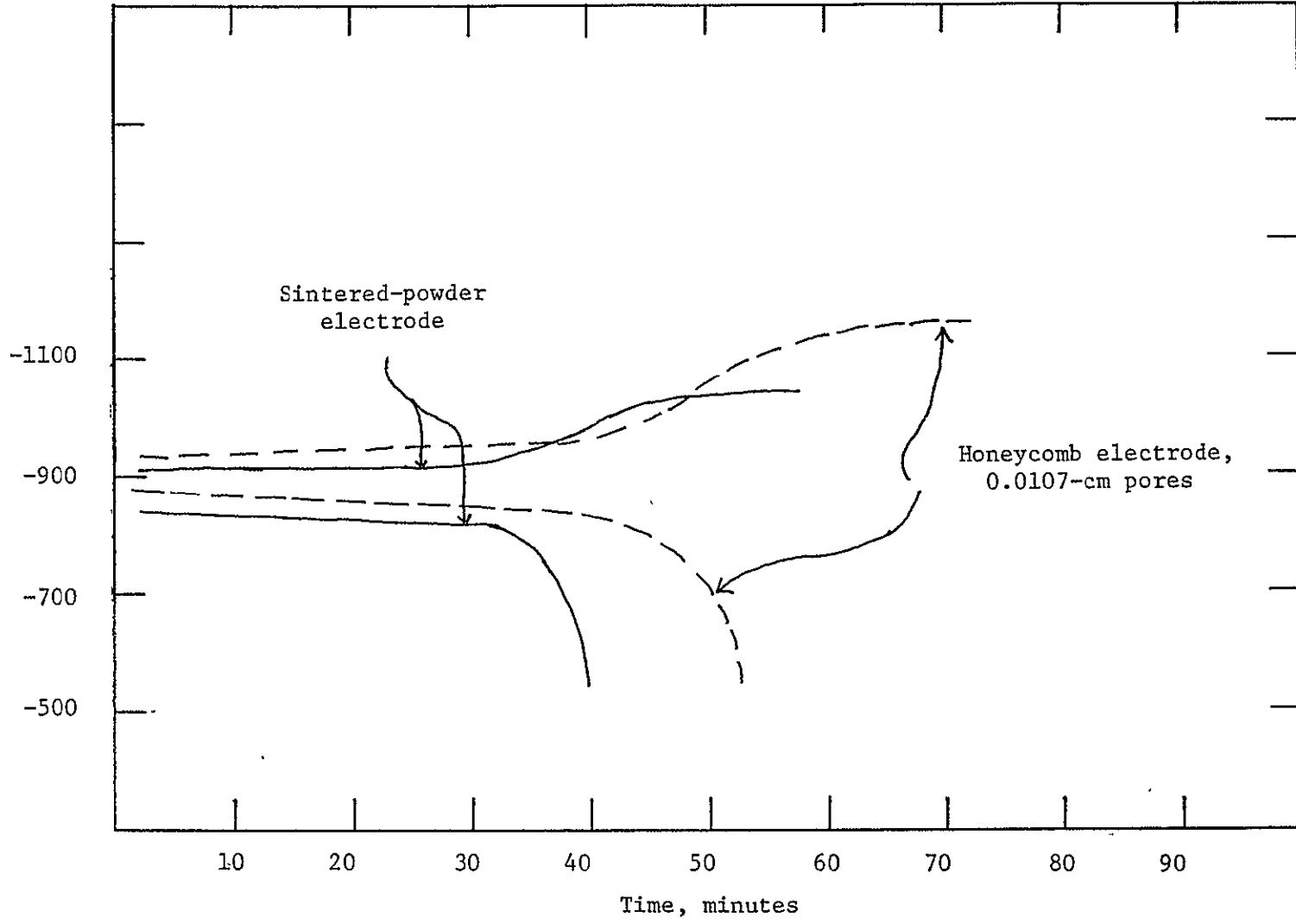


FIGURE 15. TYPICAL CHARGE AND DISCHARGE CURVE FOR SINTERED-POWDER AND HONEYCOMB ELECTRODES

Honeycomb electrode charge and discharge rates were 240 mA. Sintered-powder electrode charge and discharge rates were 280 mA.

general shape of curves that are typical of cadmium electrodes, although the honeycomb electrode has a greater potential rise when it reaches hydrogen evolution because of its smaller internal plaque-surface area. That is, at constant current, the overpotential for hydrogen evolution changes logarithmically with true surface area. This higher end-of-charge voltage could be beneficial for charge control in sealed cells if they were negative-electrode limited.

Figure 16 shows a comparison of the 4C charge-and-discharge curves for a sintered-powder electrode and a 0.0107-cm-pore-diameter honeycomb electrode. It is seen that the potentials measured with respect to a Hg/HgO reference electrode are about 10 to 15 mv lower on charge and 20 to 30 mv higher on discharge for the honeycomb electrode than for the sintered-powder electrode. Thus, electrodes made from the honeycomb plaque structure appear to have less polarization loss at high-rate operation, which allows charging and discharging at rates two to five times greater than those for sintered-powder electrodes.

Temperature Effects. The effect of temperature on the charge-discharge performances of honeycomb electrodes with 0.0061-cm, 0.0076-cm, 0.0107-cm, and 0.015-cm pore diameters and of sintered-powder electrodes was studied at three different temperatures: +10 C, -5 C, and approximately -17 C.

The test cell containing one cadmium electrode and two positive nickel electrodes was mounted inside a thermostat using methanol as a coolant. During charge at the C/2 rate = 60 mA and discharge at the C rate = 120 mA the potentials of the negative electrode were measured against a Hg/HgO reference electrode in the same solution.

Table 7 gives the electrode potentials with respect to a Hg/HgO reference at the times of 50 percent charge and 50 percent discharge for five electrodes at four different temperatures. The potentials of the honeycomb electrodes were always within 35 mv of the sintered-powder electrode, which indicates that the honeycomb electrodes have a potential-temperature curve similar to the sintered-powder electrodes at the 50 percent charge and discharge points. However, the end-of-charge potential

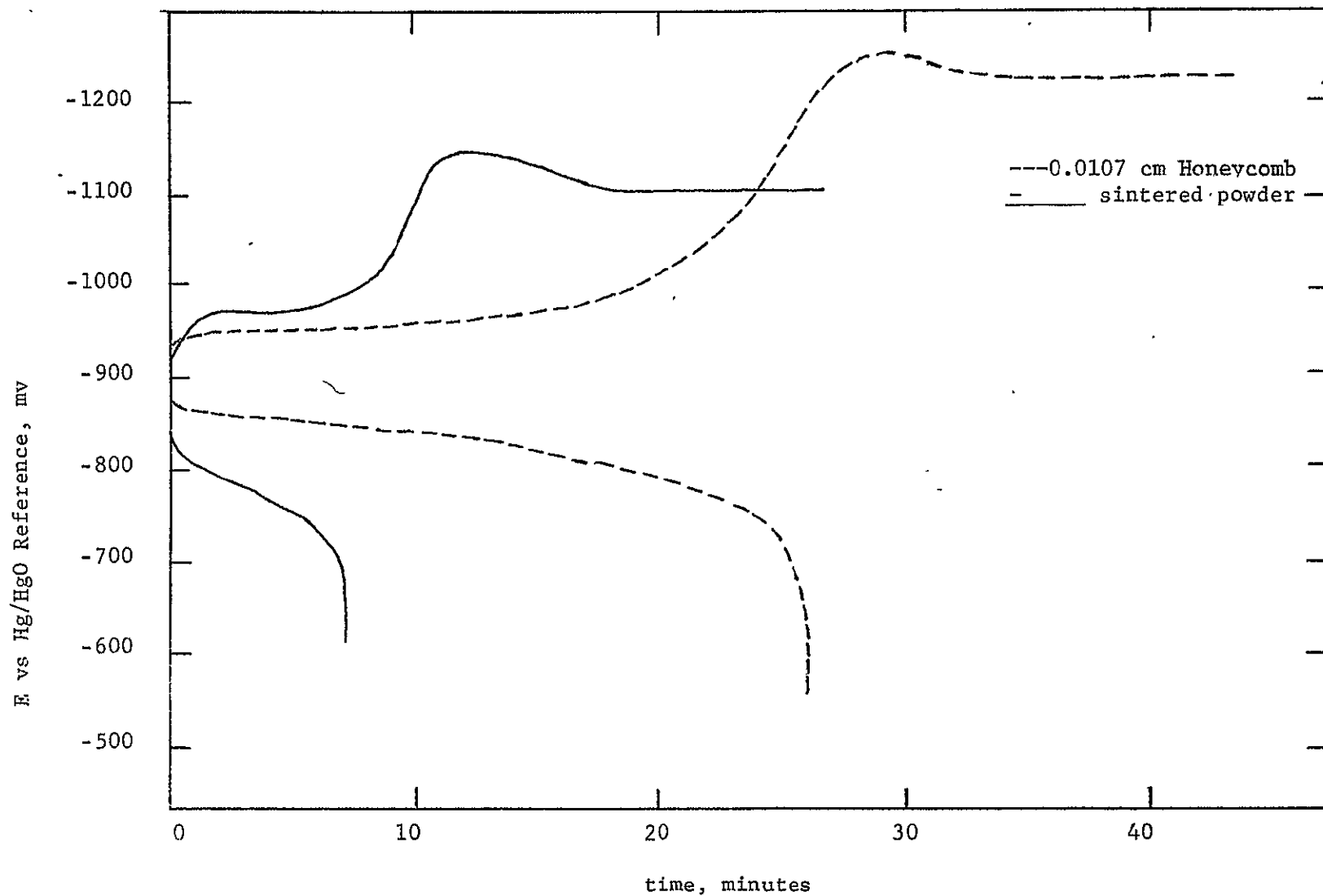


FIGURE 16. CHARGE AND DISCHARGE CURVES AT 4C RATE FOR 0.0107 CM HONEYCOMB ELECTRODE AND SINTERED POWDER ELECTRODE

differences to hydrogen evolution become less accentuated with lower temperatures with the honeycomb structure. Also, the end-of-discharge potential for the honeycomb structure changes less sharply with time as the temperature is lowered.

Table 8 gives the hydrogen-free and discharge capacities of the various electrodes obtained as a function of temperatures. These data show that the capacity of a honeycomb electrode decreases more rapidly with decreasing temperature than does the capacity of a sintered-powder electrode when both are operated at the same current. The lower discharge capacities for the honeycomb structure can be associated with a decrease in charge acceptance with decreasing temperatures.

TABLE 7. ELECTRODE POTENTIALS AS A FUNCTION OF TEMPERATURE

Type of Electrode	Temperature, C							
	25		10		-5		-17	
	Charge	Dis-charge	Charge	Dis-charge	Charge	Dis-charge	Charge	Dis-charge
Sintered Powder	-905	-840	-920	-860	-930	-875	-950	-870
0.0061-cm Honeycomb	-920	-865	-925	-860	-950	-855	-925	-855
0.0076-cm Ditto	-910	-875	-920	-830	-945	-845	-955	-840
0.0107-cm "	-920	-870	-930	-870	-950	-870	-955	-845
0.015-cm "	-920	-860	-940	-860	-955	-860	-948	-850

Oxygen Recombination. Due to a shortage of time and funds at the end of the project, only a brief, preliminary study of oxygen-recombination performance of the honeycomb electrodes was performed. Measurements were carried out in an open cell with flooded electrodes. Oxygen reduction was studied on one sintered-powder electrode and one honeycomb electrode. The

TABLE 8. ELECTRODE CAPACITY AS A FUNCTION OF TEMPERATURE
CAPACITY IN AMPERE-HOURS

Type of Electrode	Temperature, C							
	25		10		-5		-17	
	Hydrogen-Free Charge Capacity	Discharge Capacity	Hydrogen-Free Charge Capacity	Discharge Capacity	Hydrogen-Free Charge Capacity	Discharge Capacity	Hydrogen-Free Charge Capacity	Discharge Capacity
Sintered powder	0.270	0.219	0.254	0.286	0.230	0.256	0.232	0.254
0.0061-cm Honeycomb	0.263	0.210	0.213	0.188	0.224	0.188	0.135	0.134
0.0076-cm Ditto	0.147	0.142	0.184	0.126	0.114	0.112	0.087	0.080
0.0107-cm "	0.270	0.240	0.218	0.220	0.180	0.184	0.140	0.152
0.015-cm "	0.177	0.176	0.160	0.126	0.113	0.102	0.092	0.105

sintered-powder electrode was potentiostatically charged at -980 mv versus Hg/HgO reference electrode in a nitrogen-saturated electrolyte to eliminate reduction of oxygen in the electrolyte. Hydrogen evolution does not occur at this potential. When a constant current was obtained, the nitrogen was turned off and oxygen was bubbled through the electrolyte. As a result, the current increased in less than 1 minute from 2 to approximately 2.5 mA.

The same effect was measured using a precharged honeycomb electrode with a 0.0076-cm pore diameter. After bubbling nitrogen through the cell for 2 hours, oxygen was turned on and the current increased from 1 to approximately 1.5 mA at the same potential of -980 mv versus a Hg/HgO reference electrode. This simple experiment shows that oxygen reduction, which is commonly called "oxygen recombination" in the battery trade, occurs on a honeycomb electrode at a rate which is similar to that on a sintered-powder electrode in the flooded state.

While the actual current due to oxygen recombination in this experiment corresponds to a rate of about C/400 for the sintered-powder electrode and C/300 for the honeycomb electrode based on capacities given in Table 8, this is a much lower value than would actually be obtained for an electrode in a starved electrolyte condition, since it is generally recognized⁽⁸⁾ that the rate of oxygen recombination is limited by the rate of oxygen transport to the cadmium electrode, which is much lower in the flooded state than in the starved state.

Wetting Rates of Electrodes. One sintered-powder electrode and one honeycomb electrode of each pore diameter were evaluated to determine the rate at which they absorbed 30 percent KOH and the amount of electrolyte they could absorb. Dry and alkaline-free electrodes were placed horizontally on a perforated polypropylene sheet to eliminate any capillary action between the electrode and a smooth, flat support. One drop of KOH was placed with an eye dropper in the center of the electrode and the time until the drop was completely absorbed by the electrode was measured. The drop of electrolyte immediately soaked into all of the electrodes rather than lying on the surfaces and slowly soaking into them. During the measured

wetting times shown in Table 9, the drop of electrolyte was seen to spread laterally in the electrode as evidenced by an increasing wetted area and a decrease in the amount of light reflected by electrolyte film spread out on the electrode surface. The times reported in Table 9 are the times required for the drop of electrolyte to be completely absorbed by the electrode as indicated by a decrease in light reflectivity from the electrolyte film on the electrode surface. A second drop was placed on the same spot and the absorption time was measured again.

After soaking the electrode for 10 hours in 30 percent KOH solution and wiping off the excess KOH with a straight-edged rubber sheet, the absorption capacity was determined by weighing the electrodes. The data obtained from these experiments are shown in Table 9. It is seen that the rate and amount of wetting of honeycomb electrodes is similar to or higher than that obtained with sintered-powder electrodes.

TABLE 9. RATE AND AMOUNT OF WETTING OF ELECTRODES WITH 30 PERCENT KOH

Electrode Type	First Drop Absorption Time, sec	Second Drop Absorption Time, sec	Weight KOH Absorbed After 10 hours, g
Sintered powder	42.0	113	0.2564
0.0049-cm Honeycomb	22.0	29	0.2093
0.0061-cm Ditto	40.0	92	0.2205
0.0076-cm "	9.5	20	0.2578
0.0107-cm "	6.0	21	0.2564
0.015-cm "	21.5	30	0.2133

In order to compare the amounts of KOH absorbed on a uniform basis, the data from the last column of Table 9 were used to calculate the weight of KOH absorbed per unit weight of impregnated material and the weight of KOH absorbed per unit volume of electrode. The weight of active material was taken from column 3 of Table 4 and the electrode volume was calculated exclusive of coined area.

TABLE 10. ABSORBED ELECTROLYTE IN ELECTRODES

Electrode Type	Weight KOH/Electrode Volume, g/cm ³	Weight KOH/Weight Impregnated Material, g/g
Sintered powder	0.490	0.313
0.0049-cm Honeycomb	0.402	0.290
0.0061-cm Ditto	0.453	0.264
0.0076-cm "	0.443	0.321
0.0107-cm "	0.479	0.292
0.015-cm "	0.366	0.270

Corrugated-Electrode Cycling

A corrugated nickel foil 2.5 x 2.5 cm with a tab for electrical contact was cleaned and coated with 178 mg of cadmium hydroxide powder as described in the impregnation section. A cell was made by stacking the following items in sequence: one glass plate, the corrugated foil, three layers of 0.038-cm-thick Pellon 2505, one commercial positive electrode 2.5 x 2.5 cm with contact tab, and one Lucite cover plate. The assembly was clamped together with a "C" clamp and three edges were sealed with hot

wax. About 0.5 ml of 30 percent potassium hydroxide solution was added, then the last side closed with hot wax. No excess electrolyte was visible. Cycling was started as shown in Table 11, but capacity dropped after the third cycle.

TABLE 11. DISCHARGE RESULTS OF CELL CONTAINING
A CORRUGATED-FOIL ELECTRODE

Cycle	Current, ma	Time (a), Minutes	mA-hr	Utilization Efficiency ^(b) , percent
1	20	29	9.7	6.7
2	20	39	13.0	20.0
3	20	29	9.7 ^(c)	6.7 ^(c)
4	20	45	15.0	23.0
5	20	52	17.3	26.6
6	20	62	20.7	32.0
7	20	95	32.0	49.0
8	20	118	39.2	60.0
9	40	68	45.5	70.0

(a) Discharge time to a 1-volt cell cutoff. Charges were at the same current as discharges.

(b) Based on 177 mg cadmium hydroxide.

(c) More electrolyte added.

An additional 0.5 ml of electrolyte was added, the cell was reclosed with wax, and cycling was continued. After a total of nine cycles, the cell was charged, disassembled, and the electrode was examined. The weight of material on the corrugated-foil electrode was 136.5 mg, which would correspond to 178 mg of cadmium hydroxide if the 136.5 mg were metallic Cd.

Because 177 mg of cadmium hydroxide was initially applied to the electrode, most of the product on the corrugated foil was cadmium metal. The appearance of this product was of light-gray metallic powder.

Based on this experiment with the corrugated foil, it appears that a large-surface-area electrode structure is not needed to achieve utilization efficiencies of at least 70 percent. The data indicate that higher utilization efficiencies can be achieved because the values were increasing with each cycle.

Plans for Life Tests

This plan is based on knowledge gained on Contract No. NAS 5-11594--"Study of Space Battery Accelerated Testing Techniques". The Phase III Report, "Recommended Specifications for Experimental Design and Test Facilities", submitted on July 9, 1970, to NASA Goddard Space Flight Center gives detailed descriptions of five recommended accelerated life tests. The primary independent variables in these five tests are (1) environmental temperature, (2) amount of overcharge, (3) rate of charge, (4) depth of discharge, and (5) rate of discharge. It is believed that tests involving the last two independent variables will be most useful in determining the life of the cadmium electrodes made with honeycomb plaques on this project.

The tests recommended on Contract NAS5-11594 required ten cells operated at each of five values of the independent variable for each test. Five of the ten cells are to be removed from test at selected intervals for analysis to determine what changes are occurring which are leading to failure. The five values of the independent variable are required to provide statistical confidence that the failure mechanism remains unchanged over the range of the independent variable used in the test. In addition to the 50 cells to be operated for each test, an additional five uncycled cells are to be analyzed at the start of the tests to provide reference points for comparison with changes occurring in the cycled cells.

This plan, therefore, requires a minimum of 110 honeycomb-structure electrodes with the same pore size. The complete life-test plan is divided into two parts: (1) fabrication of a sufficient number of electrodes having the same pore size and (2) the actual life tests.

Electrode Fabrication. The electrodes will be fabricated according to the methods developed on this project and described earlier in this report. It is recommended that electrodes with a 0.01-cm pore diameter be used for the life test since that type of electrode appeared to have the best performance based on measurements to date.

Life Tests. The two tests planned are (1) the rate-of-discharge test and (2) the depth-of-discharge test. Each test will start with electrodes which are 90 percent charged. The electrodes will be recharged by the amount of discharge so that their net state of charge presumably will not be altered during the life tests. The charging rate to be used throughout the tests will be C/4. The criterion for failure of an electrode will be its inability to maintain a discharge potential more negative than -0.75 volt with respect to a Hg/HgO reference electrode. An electrode will be periodically removed from test as described in the Phase III Report of Contract NAS 5-11594 and it will be analyzed for its ratio of cadmium to cadmium hydroxide to determine if this ratio is changing during the course of the test. A total of five electrodes will be removed during the course of each test at each stress level.

The tabulation below shows the levels of the independent variables for each test.

<u>Depth-of-Discharge Test</u>			<u>Rate-of-Discharge Test</u>		
<u>Level</u>	<u>Depth, %</u>	<u>Rate</u>	<u>Level</u>	<u>Rate</u>	<u>Depth, %</u>
1	25.0	C/4	1	C/4	60
2	42.5	C/4	2	C/2	60
3	60.0	C/4	3	C	60
4	77.5	C/4	4	2C	60
5	95.0	C/4	5	4C	60

The depths and rates of discharge listed above refer to the capacity of the 90-percent-charged electrode. This original state of charge was chosen to simulate conditions in sealed nickel-cadmium cells in which the cadmium electrode is never supposed to become fully charged. Tests should be performed using flooded cells having one cadmium electrode and two commercial nickel hydroxide positives.

The above plan for life tests fulfills the contractual requirement of Paragraph D of Article B of the Statement of Work, which states that life tests will be planned. It seems, however, that the next logical step in developing the technology of sealed nickel-cadmium cells having honeycomb-structure electrodes would be to verify that the electrodes can be operated in the starved electrolyte condition required for sealed cells. Thus far, it has been shown that the performance of cadmium electrodes with the new plaque structures is similar to electrodes made with sintered-powder plaques as far as voltage and utilization are concerned. The major improvement in short-term cycling in the flooded state is that the new electrodes lose less capacity during cycling than do electrodes with sintered-powder plaques.

It appears that there would be an advantage to developing a complete cell with honeycomb-structure electrodes and then life test the complete cell instead of only electrodes. The honeycomb plaque structure should also be evaluated for the nickel positive electrode, because it has a smaller specific surface area than a sintered-powder plaque and therefore would be expected to show less plaque corrosion.

After complete cells with electrodes made from the new plaque structures are fabricated, it will be necessary to life test them in a manner similar to that described in the above life-test plan. By building complete cells for life tests, one can obtain a direct comparison of cell performance and life with that of conventional cells, whereas there might be no direct correlation with cell life and performance if only electrodes were life tested. The building of complete cells prior to actual life testing thus seems to be a more efficient route toward developing the technology of sealed nickel-cadmium cells with honeycomb plaques.

New Technology

Three items are considered new technology for which appropriate "new technology forms" have been submitted. These items are (1) the techniques for fabricating honeycomb plaques by electroforming corrugated and flat foils, stacking, and heat bonding; (2) electroforming exact replicas of plastic surfaces by (a) depositing a silver film, (b) electrodepositing a copper plate, (c) separating the metal from the plastic mandrel, (d) nickel plating on the silver surface, and (e) chemically dissolving the copper and the silver; and (3) the use of porous plaques with pores directly connected to the surface of the plaque, with noninnerconnecting pores, and with all pores the same size for making cadmium electrodes.

CONCLUSIONS AND RECOMMENDATIONS

The results of this work show that cadmium electrodes made from plaques with uniform, noninterconnecting pores perform similarly to cadmium electrodes using the usual sintered-powder plaques. The charge and discharge curves for cadmium electrodes made with these new honeycomb plaques have the same flat plateaus as are obtained with sintered-powder plaques. This shows that a high-internal-surface-area plaque is not essential for proper cadmium electrode performance. Furthermore, the charge-discharge performance of the electrodes is relatively insensitive to pore size. Another feature of these electrodes is the greater potential rise when the hydrogen-evolution point is reached. This change in voltage might be used as a signal to indicate a fully charged negative electrode in a cell and a dangerous condition in which excessive gas pressure could be produced if charging were continued. It seems, however, that the normal cadmium nitrate impregnation procedure requires some modification for the honeycomb plaque structures. For example, the time of polarization, or the current, or both, should be decreased.

REFERENCES

- (1) Fleischer, A., "Sintered Plates for Nickel-Cadmium Batteries", *Trans. Electrochem. Soc.*, 94 (6), 289-299 (1948).
- (2) Bailin, P., "Electroforming Automation at Columbia Records", *Plating*, 56, 658-664 (1969).
- (3) Fleischer, A., "Electric Battery Plate and Method of Producing the Same", U. S. Patent 2,771,499 (November 20, 1956).
- (4) Falk, S. U., and Salkind, A. J., Alkaline Storage Batteries, John Wiley and Sons, Inc., New York (1969), pp 131-134.
- (5) *Ibid*, p 45.
- (6) Reed, A. H., Cover, P. W., and McCallum, J., "Failure Mechanisms and Analyses of Sealed Batteries", Technical Report AFAPL-TR-69-74 (September, 1969), Wright-Patterson Air Force Base Contract No. AF 33(615)-3701, p 23.
- (7) Reference (4), p 128.
- (8) Proceedings of the Third International Symposium held at Bournemouth, October, 1962. (B-12).
- (9) Casey, Edmund J., Lake, Phyllis E., and Nagy, Gerard D., "Method of Incorporating an Electrochemically Active Cadmium Compound Into a Porous Nickel Plaque", U. S. Patent 3,068,312 (December 11, 1962). (B-114).

DISTRIBUTION LIST

No. of Copies	Addressee	Code
1	Systems Reliability Directorate	300
1	T&DS Directorate	500
1	Patent Counsel	204
1	Documentation Branch	256
1	GSFC Library	252
1	Contracting Officer	245
3	Technical Officer	735
1	Technology Directorate	700
Balance	Battery Distribution List	

1 reproducible required

DISTRIBUTION LIST

Dr. James D. Birkett
Arthur D. Little, Inc.
Acorn Park
Cambridge, Mass 02140

Dr. Per Bro
P. R. Mallory & Company, Inc
Northwest Industrial Park
Burlington, Mass 01801

Dr. George Moe
McDonnell Doug Astronautics Co
Headquarters - Space Sys Cen
Building 11-3-12 MS 12
5301 Bolsa Avenue
Huntington Beach, Calif 92647

Mr. Leon Schulman
Portable Power Sources Corp
166 Pennsylvania Avenue
Mount Vernon, New York 10552

Saft Corp of America
Attn. Mr. D. Verrier
50 Rockefeller Plaza
New York, N. Y. 10020

Dr. Fritz R. Kalhammer
Stanford Research Institute
19722 Jamboree Blvd.
Irvine, California 92664

TRW Inc.
Attn. Librarian TIM 3417
23555 Euclid Avenue
Cleveland, Ohio 44117.

Dr. Robert Powers
Consumer Products Division
Union Carbide Corporation
P. O. Box 6116
Cleveland, Ohio

The Librarian
Livingston Electronic Lab
Honeywell Incorporated
Montgomeryville, Pa. 18936

P. R. Mallory & Company, Inc.
Library
P. O. Box 1115
Indianapolis, Indiana 46206

Dr. John Mauchly
Mauchly Associates, Inc.
Commerce and Enterprise
Montgomeryville, Pa. 18936

Power Information Center
University City Science Ins
3401 Market Street, Room 2107
Philadelphia, Penn 19104

Mr. A. Mundel
Sonotone Corporation
Saw Mill River Road
Elmsford, New York 10523

Dr. J. W. Ross
Texas Instruments, Inc.
34 Forest Street
Attleboro, Mass 02703

Dr. Jose Giner
Tyco Laboratories, Inc.
Bear Hill
Hickory Drive
Waltham, Massachusetts 02154

Mr. William Boyd
Utah Research and Development
1820 South Industrial Road
Salt Lake City, Utah 84104

DISTRIBUTION LIST

(Continued)

Mr. L. K. White
Whittaker Corporation
3850 Olive Street
Denver, Colorado 80207

Dr. H. L. Recht
Atomics International Division
North American Aviation, Inc.
P. O. Box 309
Canoga Park, California 91304

Mr. D. O. Feder
Bell Telephone Labs, Inc.
Murray Hill, New Jersey 07974

Dr. Eugene Willihnganz
C & D Batteries
Division of Eltra Corporation
3043 Walton Road
Plymouth Meeting, Penn 19462

Dr. L. J. Minnich
G & W. H. Corson, Inc.
Plymouth Meeting, Penn 19462

Director of Engineering
ESB, Inc.
P. O. Box 11097
Raleigh, North Carolina 27604

Mr. R. H. Sparks
Electromite Corporation
2117 South Anne Street
Santa Ana, California 92704

Dr. Arthur Fleischer
466 South Center Street
Orange, New Jersey 07050

General Electric Company
Attn. Whitney Library
P. O. Box 8
Schenectady, New York 12301

Mr. P. Deluca & Mr. Mike Read
Yardney Electric Company
82 Mechanic Street
Pawcatuck, Conn 02891

Mr. R. F. Fogle, GF 18
Autometics Division, NAR
P. O. Box 4181
Anaheim, California 92803

Dr. Carl Berger
13401 Kootenay Drive
Santa Ana, California 92705

Professor T. P. Dirkse
Calvin College
3175 Burton Street, S. E.
Grand Rapids, Michigan 49506

The Librarian
Cubic Corporation
9233 Balboa Avenue
San Diego, Calif 92123

Dr. Galen Frysinger
ESB, Inc.
Carl F. Norberg Research Cen
19 West College Avenue
Yardley, Pennsylvania 19067

Dr. W. P. Cadogan
Emhart Corporation
Box 1620
Hartford, Connecticut 06102

Dr. R. P. Hamlen
Research and Development Cen
General Electric Company
P. O. Box 43
Schenectady, New York 12301

DISTRIBUTION LIST

(Continued)

Grumman Aerospace Corporation
OAR PROJ /S. J. Gaston, PL 41/
Bethpage, Long Island
New York 11714

Dr. H. T. Francis
IIT Research Institute
10 West 35th Street
Chicago, Illinois 60616

Mr. N. A. Matthews
International Nickel Company
1000-16th Street, N.W.
Washington, D.C. 20036

NASA
National Aero
and Space Admin
Scientific and Technical
Information Center. Input
P. O. Box 33
College Park, Maryland 20740

Mr. Richard Livingston,
Code MTG
National Aero
and Space Admin
Washington, D.C. 20546

Mr. Joseph Sherfey Code 734
Goddard Space Flight Center
National Aero
and Space Admin (20)
Greenbelt, Maryland 20771

Dr. Louis Rosenblum, MS 302-1
Lewis Research Center
National Aero
and Space Admin
2100 Brookpark Road
Cleveland, Ohio 44135

Mr. David F. Schmidt
General Electric Company
777-14th Street N.W.
Washington, D.C. 20005

Battery and Power Sources Div
Gulton Industries
212 Durham Avenue
Metuchen, New Jersey 08840

Dr. G. Myron Arcand
Department of Chemistry
Idaho State University
Pocatello, Idaho 83201

Mr. Richard E. Evans
Applied Physics Laboratory
Johns Hopkins University
8621 Georgia Avenue
Silver Spring, Maryland 20910

Mr. Ernst M. Cohn, Code RNW
National Aero
and Space Admin
Washington, D.C. 20546

Mr. Jon Rubenzer, M.S. 244-2
Ames Research Center Code PBS
National Aero
and Space Admin
Moffett Field, Calif 94035

Mr. Louis Wilson, Code 450
Goddard Space Flight Center
National Aero
and Space Admin
Greenbelt, Maryland 20771

Mr. Harvey Schwartz, MS 309-1
Lewis Research Center
National Aero
and Space Admin
21000 Brookpark Road
Cleveland, Ohio 44135

DISTRIBUTION LIST

(Continued)

Mr. W. E. Rice, EP5
Manned Spacecraft Center
National Aero
and Space Admin
Houston, Texas 77058

Mr. Nathan Kaplan
Harry Diamond Laboratories
Room 300, Building 92
Conn Ave. & Van Ness St., N.W.
Washington, D.C. 20438

Mr. Leo A. Spano
Clothing & Organic Mats Div.
U. S. Army Natick Laboratories
Arlington, Virginia 22217

Mr. J. H. Harrison, Code A731
Naval Ship R&D Laboratory
Annapolis, Maryland 21402

Mr. C. F. Viglotti, 6157D
Naval Ship Engineering Center
Center Bldg, Prince Geo Center
Hyattsville, Maryland 20782

Mr. Ed Raskind, CREC, Wing F
AF Cambridge Research Lab
L. G. Hanscom Field
Bedford, Massachusetts 01731

Aerospace Corporation
Attn. Library Acquisition GR
P. O. Box 95085
Los Angeles, California 90045

Dr. John McCallum
Battelle Memorial Institute
505 King Avenue
Columbus, Ohio 43201

Mr. Daniel Runkle, MS 198-220
Jet Propulsion Laboratory
4800 Oak Grove Drive
Pasadena, California 91103

U. S. Army
Electro Technology Laboratory
Energy Conversion Research Div
MERDC
Fort Belvoir, Virginia 22060

Director Power Program
Code 473
Office of Naval Research
Arlington, Virginia 22217

Mr. Milton Knight, Air 340C
Naval Air Systems Command
Department of the Navy
Washington, D. C. 20360

Mr. Robert E. Trumbule, STIC
4301 Suitland Road
Suitland, Maryland 20390

Mr. Frank J. Mollura, EMRED
Rome Air Development Center
Griffiss AFB, New York 13440

Dr. R. A. Haldeman
American Cyanamid Company
1937 West Main Street
Stamford, Connecticut 06902

Mr. B. W. Moss
Bellcomm, Inc.
955 Lenfant Plaza, S. W.
Washington, D. C. 20024

DISTRIBUTION LIST

(Continued)

Mr. Sidney Gross
Mail Stop 88-06
The Boeing Company
P. O. Box 3999
Seattle, Washington 98124

Mr. F. Tepper
Catalyst Research Corporation
6308 Blair Hill Lane
Baltimore, Maryland 21209

Mr. J. A. Keralla
Delco Remy Division
General Motors Corporation
2401 Columbus Avenue
Anderson, Indiana 46011

Mr. E. P. Broglio
Eagle-Picher Industries, Inc.
P. O. Box 47, Couples Depart
Joplin, Missouri 64801

Dr. H. G. Oswin
Energetics Science, Inc.
4461 Bronx Blvd.
New York, New York 10470

Mr. K. L. Hanson
Space Systems, Room M2700
General Electric Company
P. O. Box 8555
Philadelphia, Penn 19101

Mr. John R. Thomas
Globe-Union, Inc.
P. O. Box 591
Milwaukee, Wisconsin 53201

Dr. P. L. Howard
Centreville, Maryland 21617

Mr. M. E. Wilke, Chief Eng
Burgess Battery Division
Gould, Inc.
Freeport, Illinois 61032

Mr. Robert Strauss
Communications Satellite Corp
Comsat Laboratories
P. O. Box 115
Clarksburg, Maryland 20734

Mr. J. M. Williams
Experimental Sta, Building 304
Engineering Materials Lab
E. I. duPont deNemours & Co
Wilmington, Delaware 19898

Dr. Morris Eisenberg
Electrochemical Corporation
1140 OBrien Drive
Menlo Park, Calif 94025

Mr. Martin Klein
Energy Research Corporation
15 Durant Avenue
Bethel, Connecticut 06801

Mr. P. R. Voyentzie
Bettry Business Section
General Electric Company
P. O. Box 114
Gainesville, Florida 32601

Dr. J. E. Oxley
Gould Ionics, Inc.
P. O. Box 1377
Canoga Park, California 91304

Mr. M. E. Ellison
Building 366, MS 524
Hughes Aircraft Corporation
El Segundo, California 90245

DISTRIBUTION LIST

(Continued)

Mr. R. Hamilton
Institute for Defense Analyses
400 Army-Navy Drive
Arlington, Virginia 22202

Dr. R. Briceland
Institute for Defense Analyses
400 Army-Navy Drive
Arlington, Virginia 22202

Dr. A. Moos
Leesona Moos Laboratories
Lake Success Park, Community D
Great Neck, New York 11021

Dr. Richard A. Wynveen, Pres
Life Systems, Incorporated
23715 Mercantile Road
Cleveland, Ohio 44122

Mr. Robert E. Corbett
Department 62-25, Building 157
Lockheed Aircraft Corporation
P. O. Box 504
Sunnyvale, California 94088

Mr. R. R. Glune
Mallory Battery Company
50 Broadway & Sunnyside Lane
Tarrytown, New York 10591

William B. Collins, MS 1620
and M. S. Imamura, MS F8845
Martin-Marietta Corporation
P. O. Box 179
Denver, Colorado 80201

Mr. A. D. Tonelli, MS 17 B 22
McDonnell Douglas Astro Co.
5301 Bolsa Avenue
Huntington Beach, Calif 92647

Rocketdyne Division
North American Rockwell Corp
Attn Library
6633 Canoga Avenue
Canoga Park, California 91304

Mr. D. C. Briggs
Power and Control Engineering
Department, MS R 26
Philco-Ford Corporation
3939 Fabian Way
Palo Alto, California 94303

Prime Battery Corporation
15600 Cornet Street
Santa Fe Springs, Cal 90670

RAI Research Corporation
225 Marcus Blvd.
Hauppauge, L.I., N Y 11787

Southwest Research Institute
Attn Library
P. O. Drawer 28510
San Antonio, Texas 78228

Dr. Harvey Seiger
Spectrolab Incorporated
12484 Gladstone Avenue
Sylmar, Calif 91342

Dr. W. R. Soctt /M 2/2154/
TRW Systems, Inc.
One Space Park
Redondo Beach, Calif 90278

Dr. Herbert P. Silverman
/R-1/2094/
TRW Systems, Inc.
One Space Park
Redondo Beach, California
90278

DISTRIBUTION LIST

(Continued)

Dr. Ralph Brodd
Consumer Products Division
Union Carbide Corporation
P. O. Box 6116
Cleveland, Ohio 44101

Union Carbide Corporation
Development Laboratory
P. O. Box 6056
Cleveland, Ohio 44101

Professor John O. M. Bockris
Electrochemistry Laboratory
University of Pennsylvania
Philadelphia, Penn 19104

Dr. C. C. Hein, Contract Admin
Research and Development Cent
Westinghouse Electric Corp
Churchill Borough
Pittsburgh, Penn 15235

Dr. A. M. Greg Andrug,
Code SCC
National Aero
and Space Admin
Washington, D.C. 20546

Dr. E. N. Case, Code UT
National Aero
and Space Admin
Washington, D.C. 20546

Mr. Gerald Halpert Code 734
Goddard Space Flight Center
National Aero
and Space Admin
Greenbelt, Maryland 20771

Mr. Thomas Hennigan,
Code 761.2
Goddard Space Flight Center
National Aero
and Space Admin
Greenbelt, Maryland 20771

Mr. Jack E. Zanks, MS 488
Langley Research Center
National Aero
and Space Admin
Hampton, Virginia 23365

Mr. John L. Patterson, Code 472
Langley Research Center
National Aero
and Space Admin
Hampton, Virginia 23365

Mr. J. Stuart Fordyce,
MS 309-1.
Lewis Research Center
National Aero
and Space Admin
21000 Brookpark Road
Cleveland, Ohio 44135

Mr. Chas B. Graff, S&E-ASTR-EP
Geo C. Marshall Space Fl Cen
National Aero
and Space Admin
Huntsville, Alabama 35812

Mr. Aiji Uchiyama, MS 198-220
Jet Propulsion Laboratory
4800 Oak Grove Drive
Pasadena, California 91103

Dr. R. Lutwack, MS 198-220
Jet Propulsion Laboratory
4800 Oak Grove Drive
Pasadena, California 91103

DISTRIBUTION LIST

(Continued)

Harry Diamond Laboratories
Room 300, Building 92
Connecticut Avenue & Van Ness NW
Washington, D.C. 20438

Mr. Harry W. Fox, Code 472
Office of Naval Research
Arlington, Virginia 22217

Commanding Officer
Naval Ammunition Depot
/13022, Mr. D. G. Miley/
Crane, Indiana 47522

Mr. B. B. Rosenbaum, Code 03422
Naval Ship Systems Command
Washington, D.C. 20360

Hq SAMSO
/SMTAE/Lt. R. Ballard/
Los Angeles Air Force Station
Los Angeles, California 90045

Mr. R. A. Knight
AMF Incorporated
689 Hope Street
Stamford, Connecticut 06907

U.S. Army Electronics Command
Attn. AMSEL-KL-P
Fort Monmouth, New Jersey 07703

Dr. J. C. White, Code 6160
Naval Research Laboratory
4555 Overlook Avenue, S.W.
Washington, D.C. 20360

Mr. Phillip B. Cole, Code 232
Naval Ordnance Laboratory
Silver Springs, Maryland 20910

Mr. James E. Cooper, APIP-1
Aero Propulsion Laboratory
Wright-Patterson Air Force Base
Ohio 45433

Dr. W. J. Hamer
National Bureau of Standards
Washington, D.C. 20234

Dr. R. T. Foley
Chemistry Department
American University
Mass and Nebraska Aves., N.W.
Washington, D.C. 20016